RBRC
RIKEN BNL Research Center

RHIC BEAM ENERGY SCAN PHASE II AND ITS EXPLORATION OF THE QCD PHASE DIAGRAM

CHUN SHEN

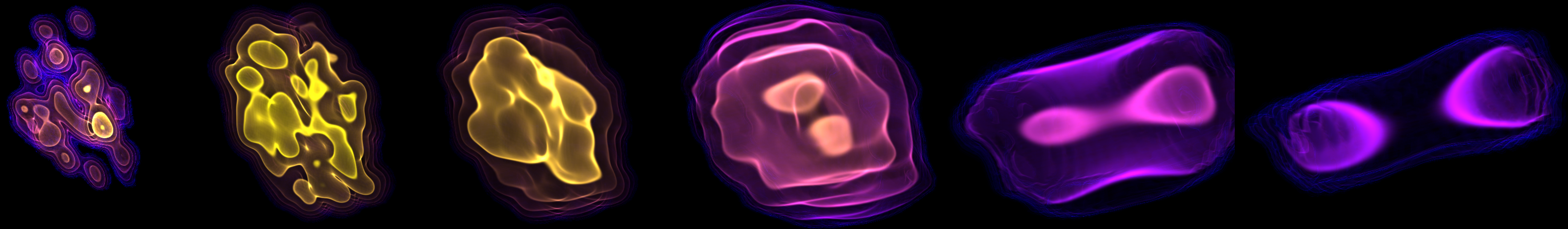

APS GHP meeting
April 14, 2021

PROBING THE NUCLEAR MATTER PHASE DIAGRAM

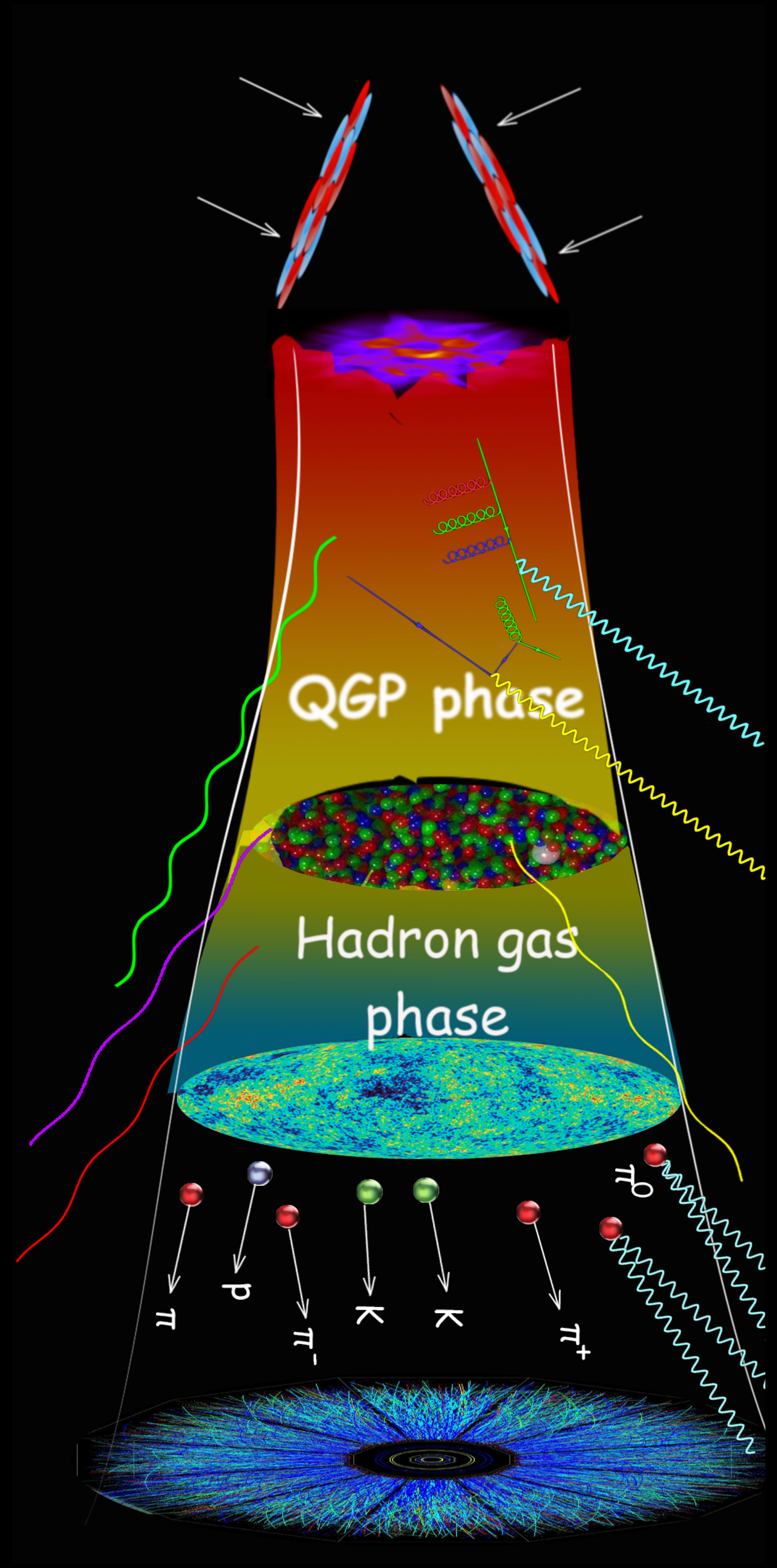

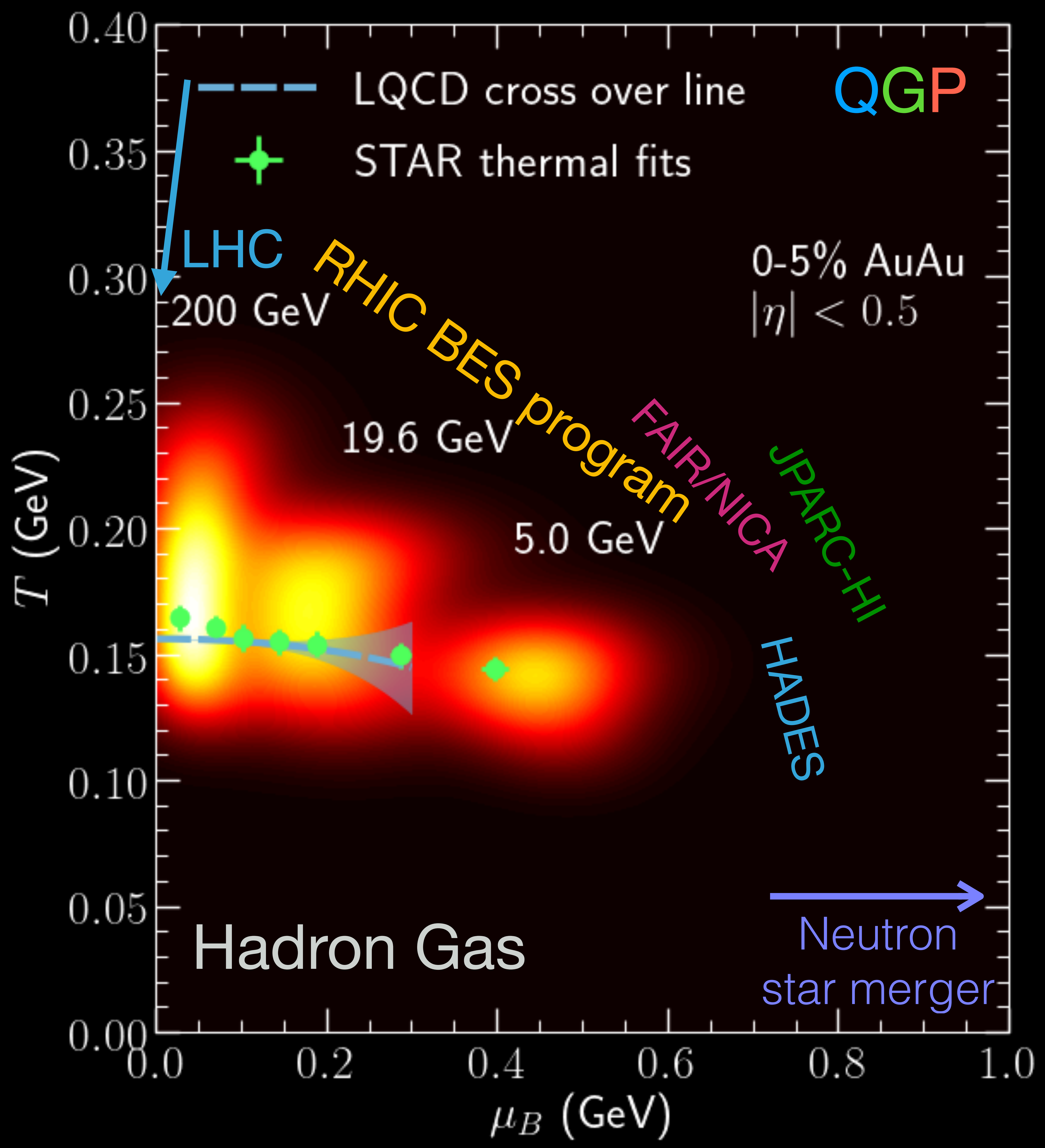

- Search for a critical point & 1st order phase transition
- How does the QGP transport property change with baryon doping?

$(\eta/s)(T, \{\mu_q\})$, $(\zeta/s)(T, \{\mu_q\})$

- Access to new transport phenomena

Charge diffusion

PROBING THE NUCLEAR MATTER PHASE DIAGRAM

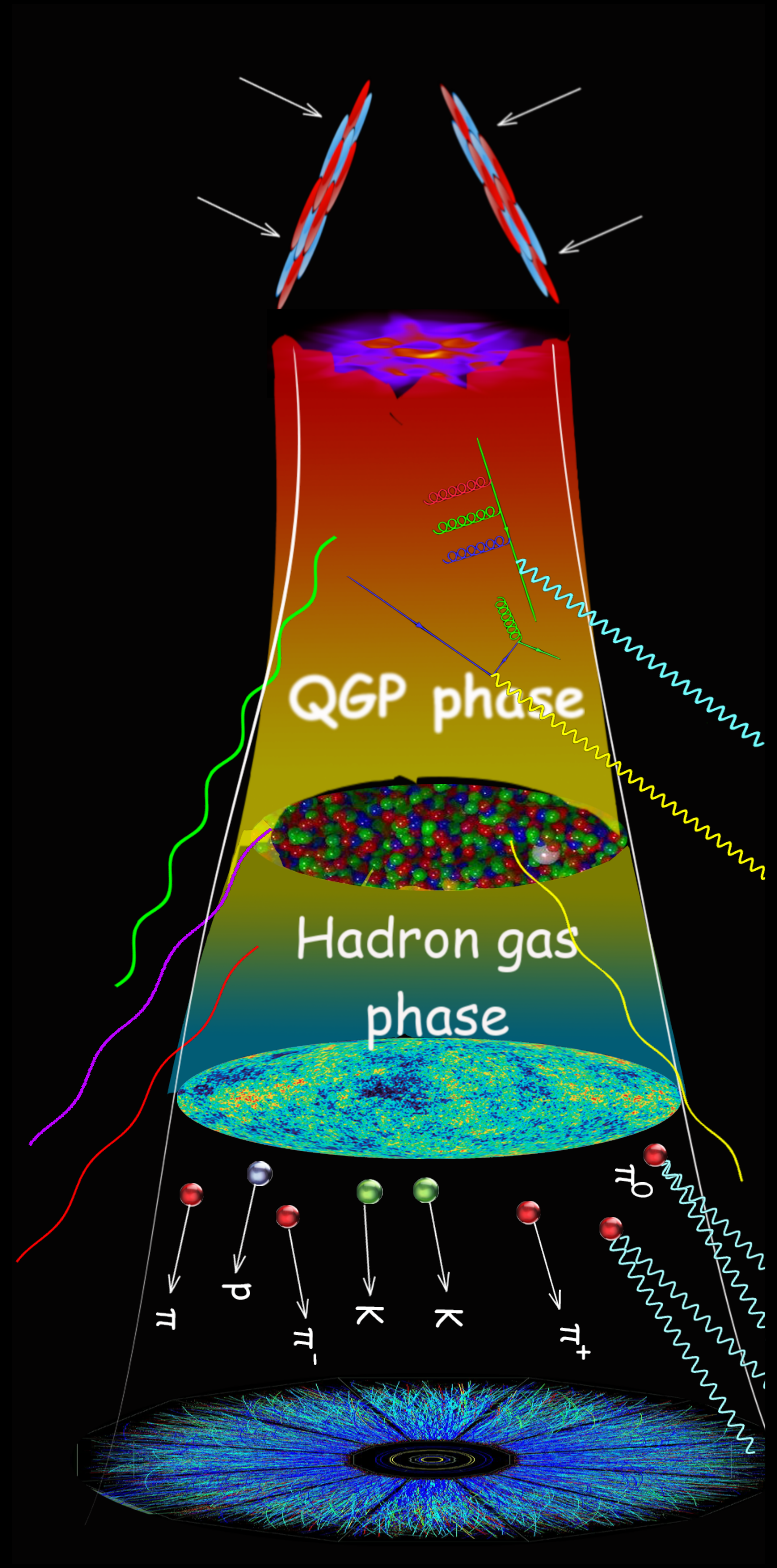

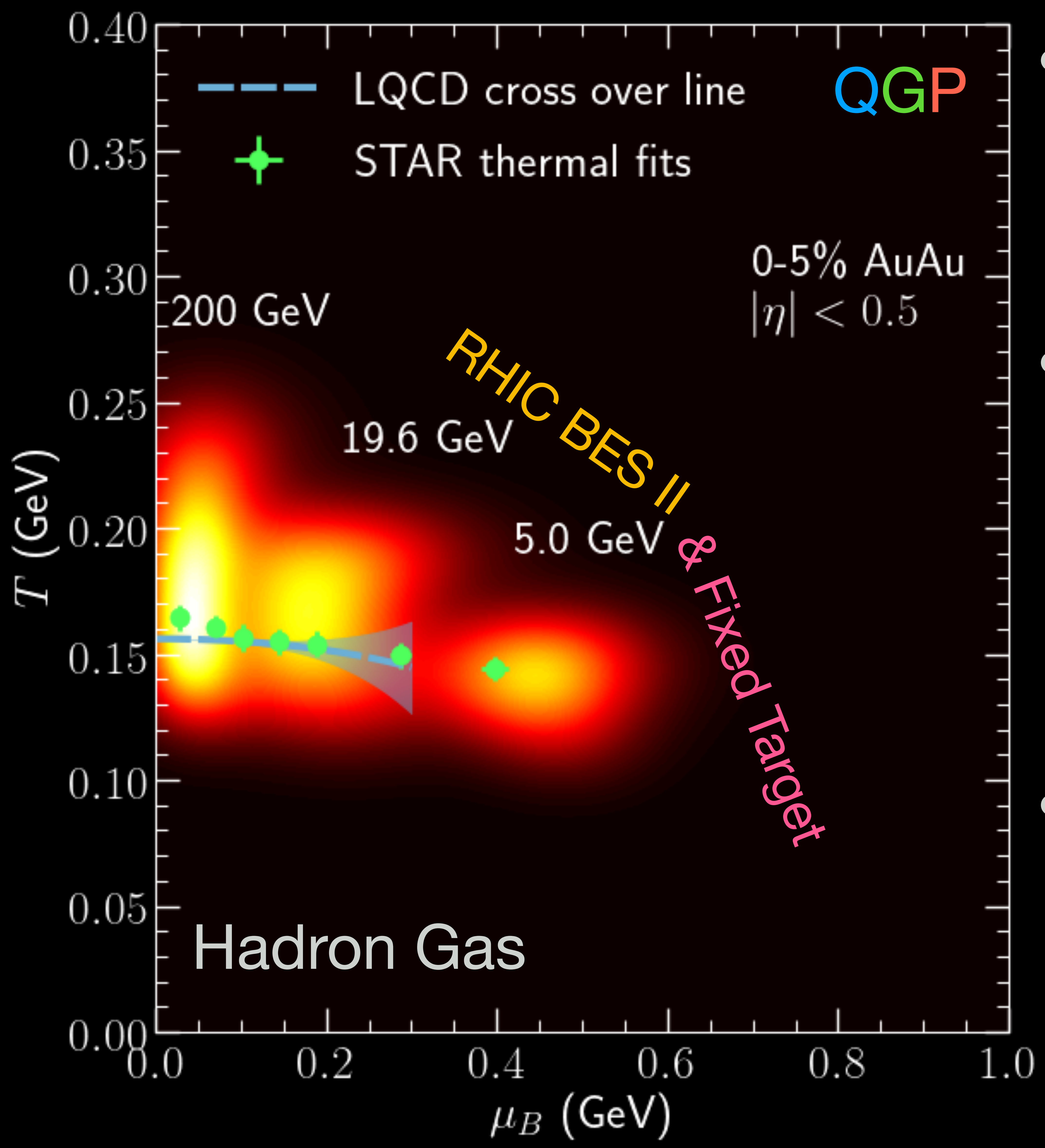

- Run 2019:
  - Collider: 14.6, 19.6, 200 GeV
  - Fixed target: 3.2 GeV
- Run 2020:
  - Collider: 9.2, 11.5 GeV
  - Fixed target: 3.5, 3.9, 4.5, 5.2, 6.2, 7.2, 7.7 GeV
- Run 2021:
  - Collider: 7.7 GeV

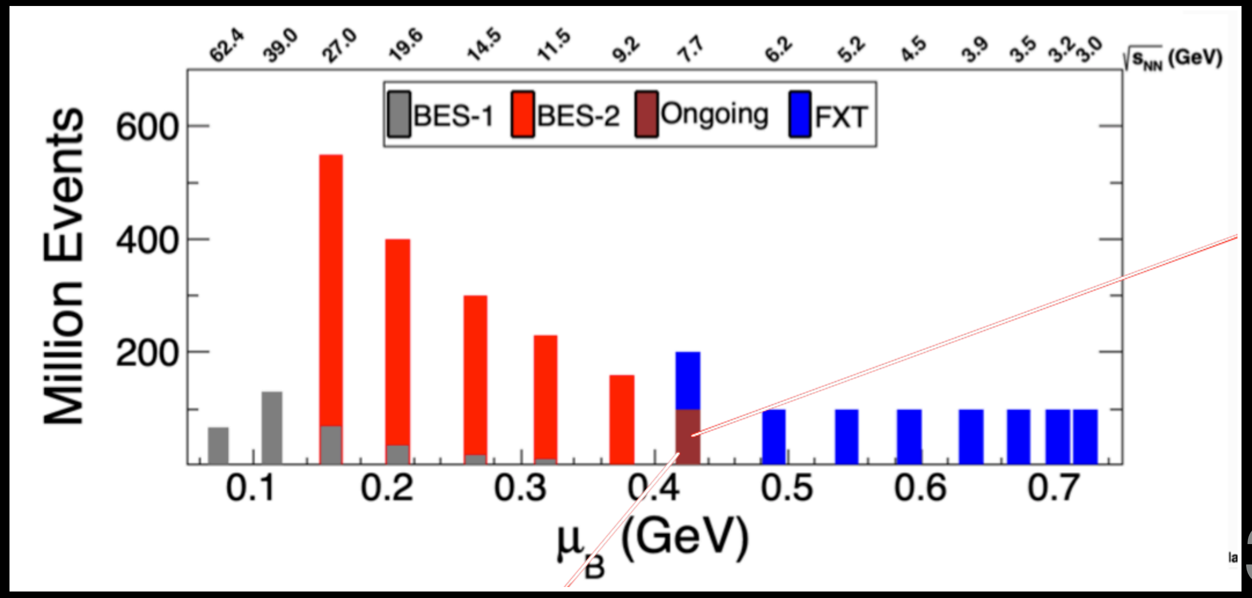

3D DYNAMICS BEYOND THE BJORKEN PARADIGM

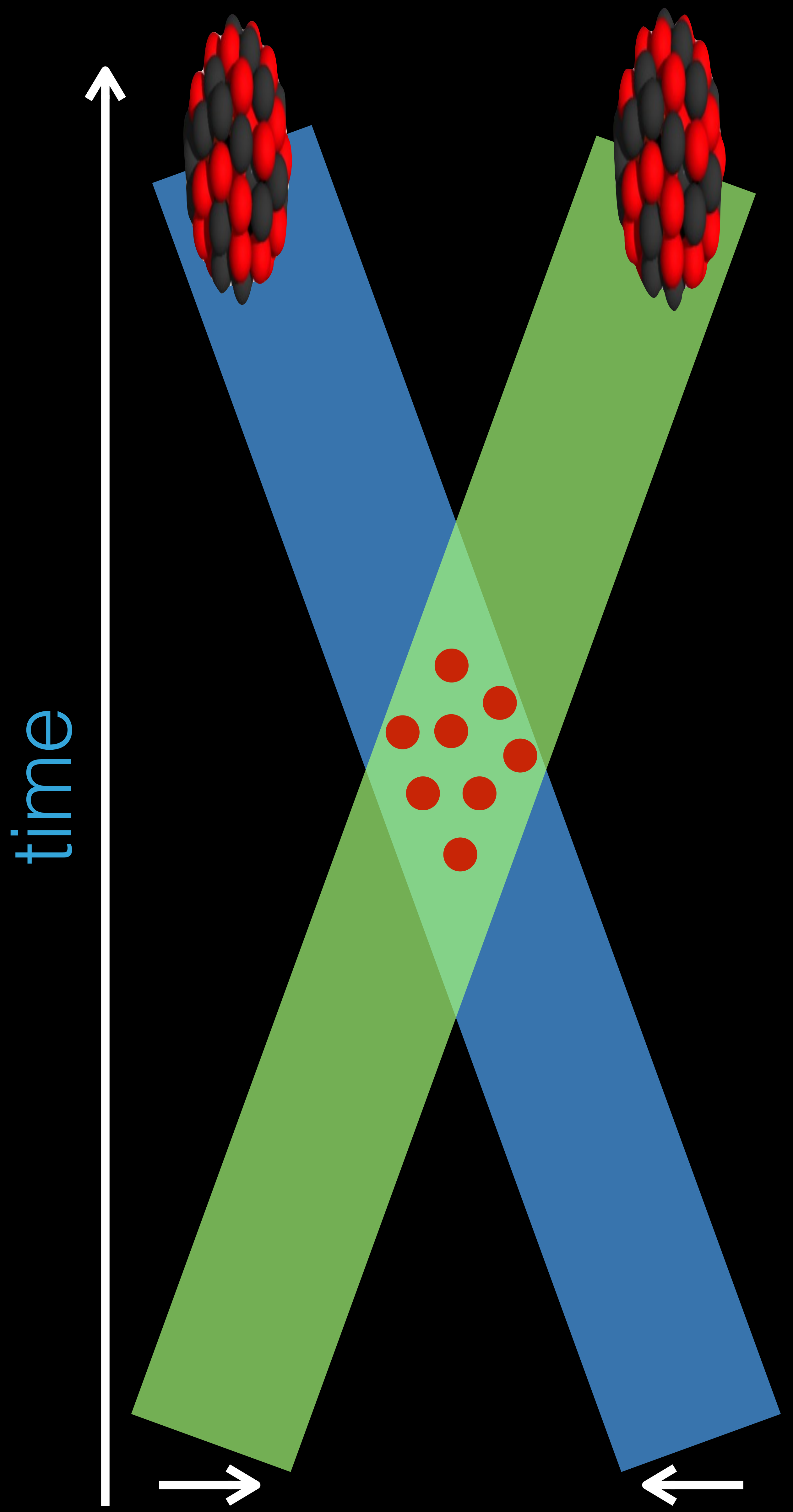

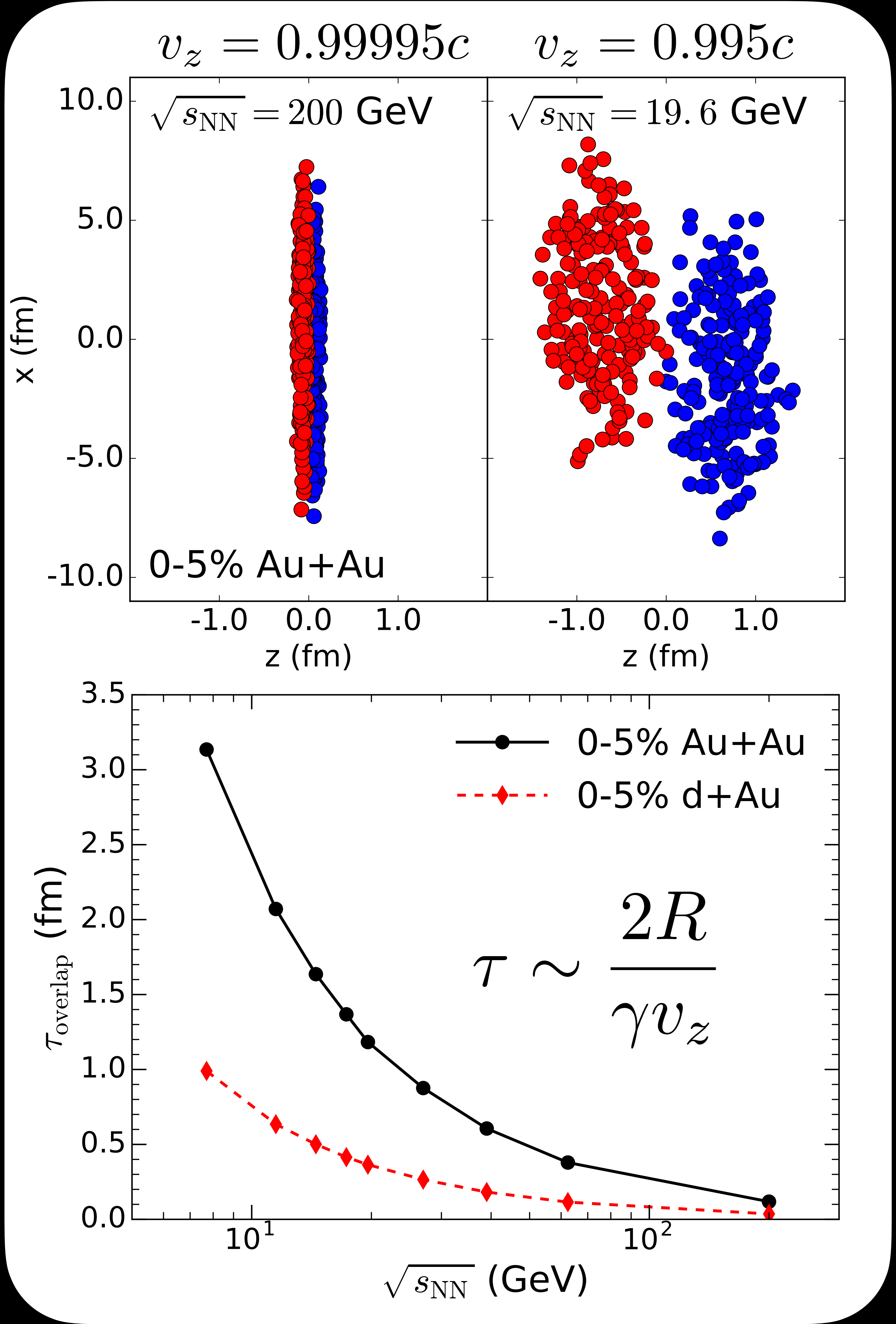

- Geometry-Based initial conditions
  - C. Shen and S. Alzhrani, Phys. Rev. C 102, 014909 (2020)
- Classical string-based initial conditions
  - A. Bialas, A. Bzdak and V. Koch, Acta Phys. Polon. B49 (2018)
  - C. Shen and B. Schenke, Phys.Rev. C97 (2018) 024907
- Transport model based initial conditions
  - I. A. Karpenko, P. Huovinen, H. Petersen and M. Bleicher, Phys. Rev. C91 (2015) 064901
  - L. Du, U. Heinz and G. Vujanovic, Nucl. Phys. A982 (2019) 407-410
- Color Glass Condensate based models
  - M. Li and J. Kapusta, Phys. Rev. C 99, 014906 (2019)
  - L. D. McLerran, S. Schlichting and S. Sen, Phys. Rev. D 99, 074009 (2019)
  - M. Martinez, M. D. Sievert, D. E. Wertepny and J. Noronha-Hostler, arXiv:1911.10272 + arXiv:1911.12454 [nucl-th]
- Holographic approach at intermediate coupling
  - M. Attems, et al., Phys.Rev.Lett. 121 (2018), 261601

HYDRODYNAMICS WITH SOURCES

Energy-momentum current and net baryon density are fed into hydrodynamic simulations as source terms

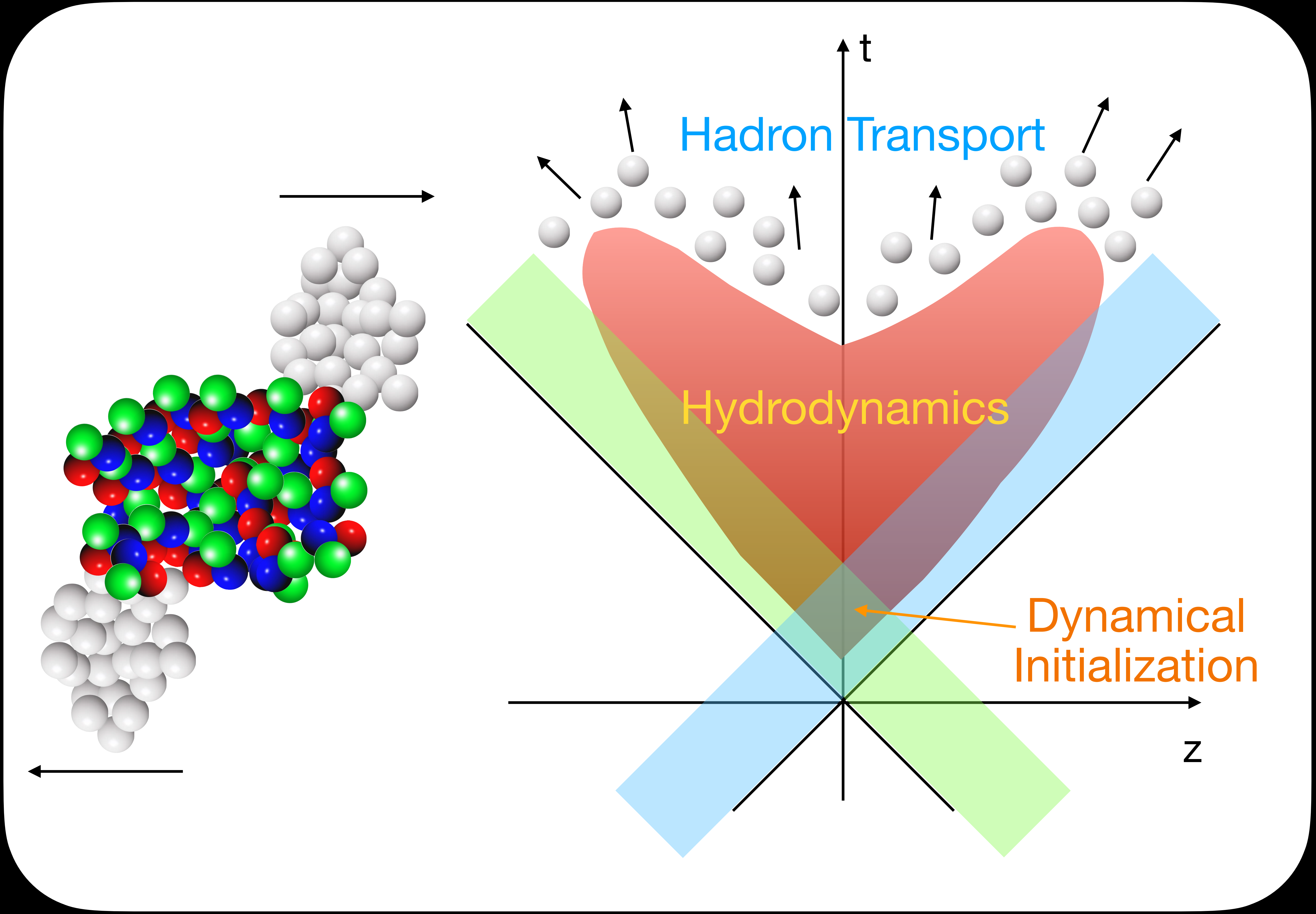

$$\partial_\mu T^{\mu\nu} = J^\nu_{\rm source}$$

$$\partial_\mu J^\mu = \rho_{\rm source}$$

M. Okai, K. Kawaguchi, Y. Tachibana, and T. Hirano, Phys. Rev. C95, 054914 (2017)

C. Shen and B. Schenke, Phys. Rev. C97 (2018) 024907

L. Du, U. Heinz and G. Vujanovic, Nucl. Phys. A982 (2019) 407-410

Y. Akamatsu, M. Asakawa, T. Hirano, M. Kitazawa, K. Morita, K. Murase, Y. Nara, C. Nonaka and A. Ohnishi, Phys. Rev. C98, 024909 (2018)

RELATIVISTIC HEAVY-ION COLLISIONS

0-5% AuAu@19.6 GeV

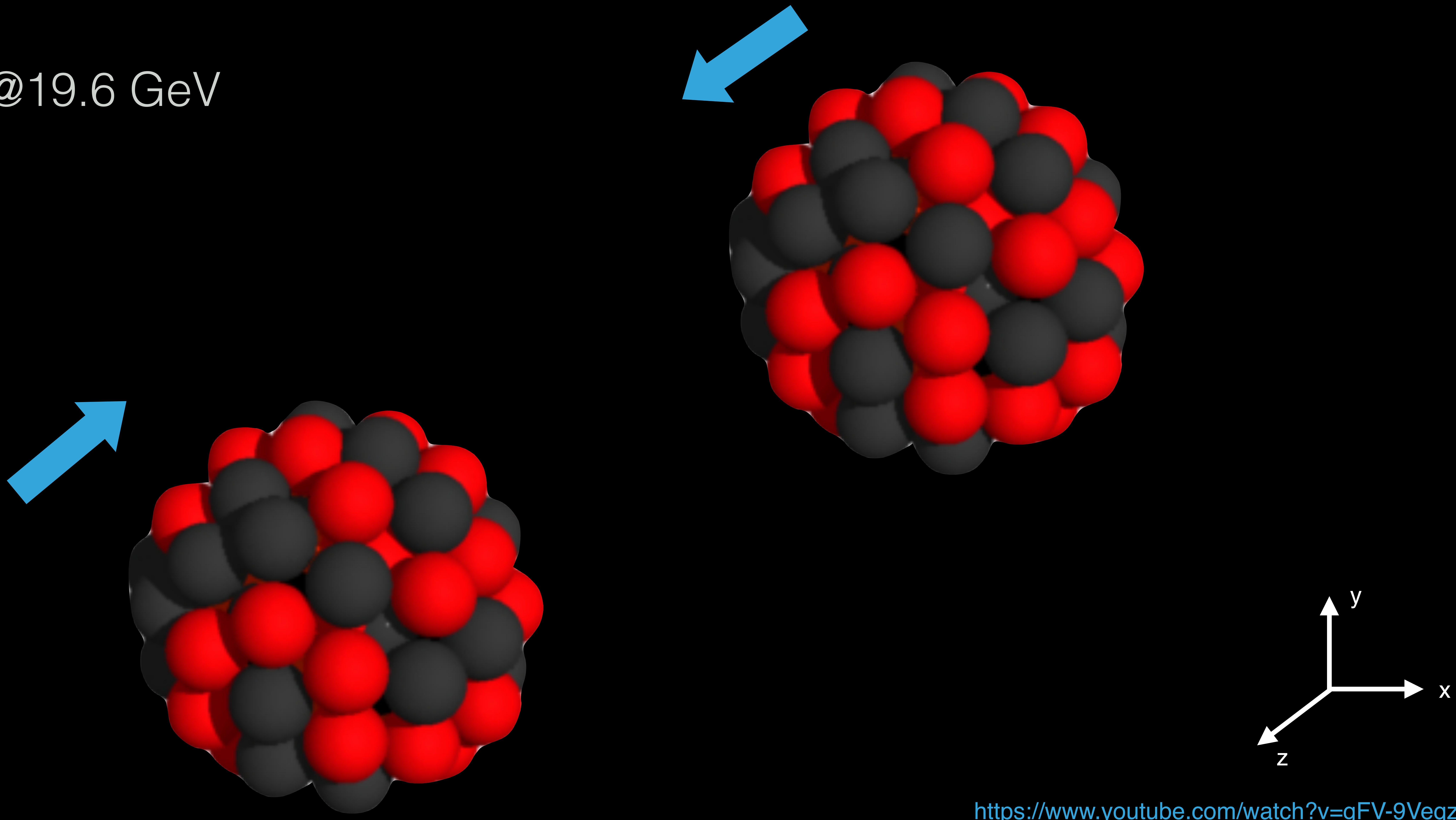

https://www.youtube.com/watch?v=gFV-9VeqzkE

FLOWING THROUGH THE QCD CROSSOVER REGION

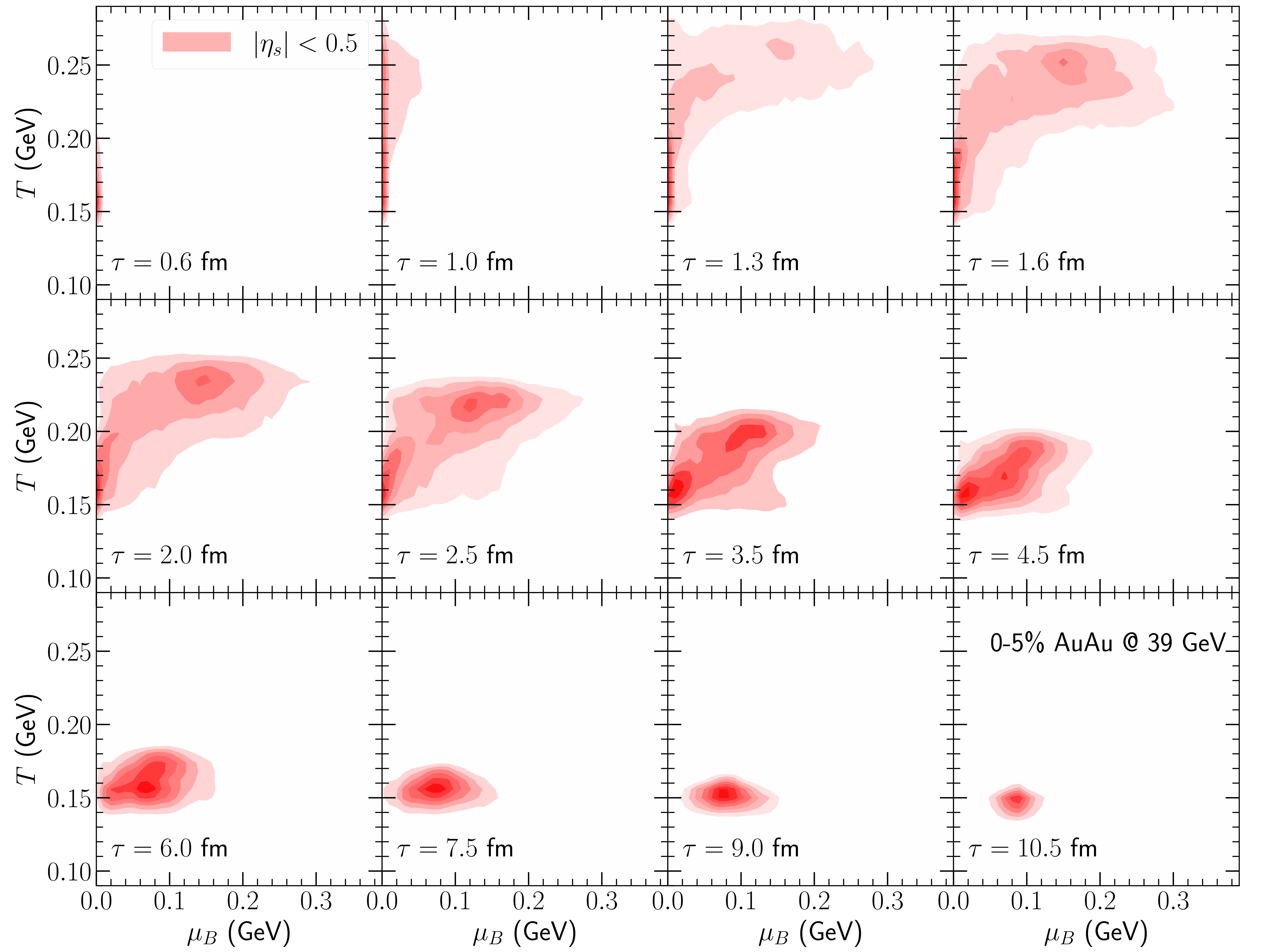

Nuclei overlap
Dynamical Initialization stage
Baryon dopping

Hydrodynamics evolution

Switching to hadronic transport

FLOWING THROUGH THE QCD CROSSOVER REGION

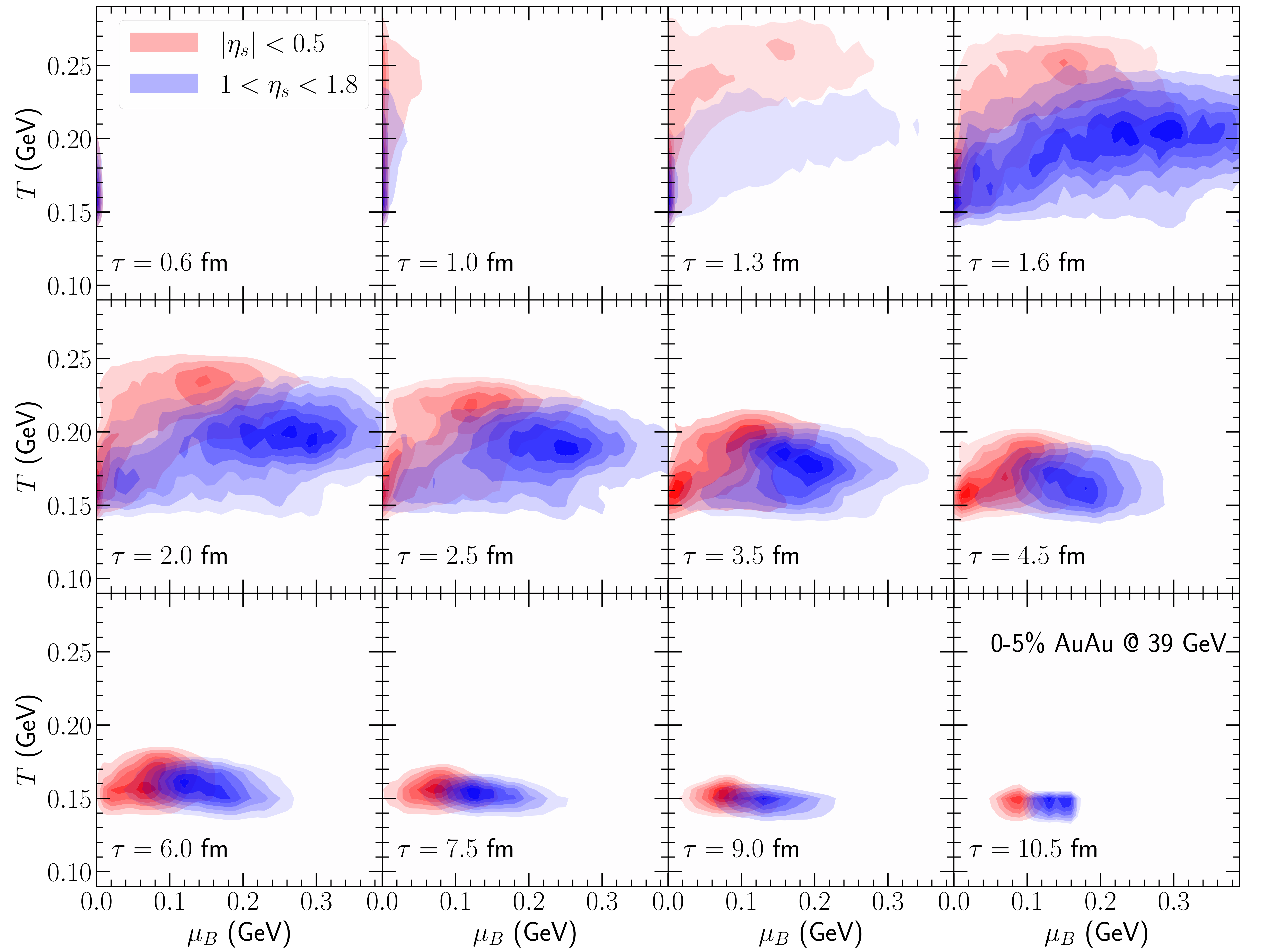

Nuclei overlap
Dynamical Initialization stage
Baryon dopping

Hydrodynamics evolution

Switching to hadronic transport

QCD EQUATION OF STATE AT FINITE DENSITIES

M. Albright, J. Kapusta and C. Young, Phys. Rev. C90, 024915 (2014)
A. Monnai, B. Schenke and C. Shen, Phys. Rev. C100, 024907 (2019)
J. Noronha-Hostler, P. Parotto, C. Ratti and J. M. Stafford, Phys. Rev. C100, 064910 (2019)
J. M. Stafford *et. al*, arXiv:2103.08146 [hep-ph]

$$n_s = 0 \quad n_Q = 0.4 n_B$$

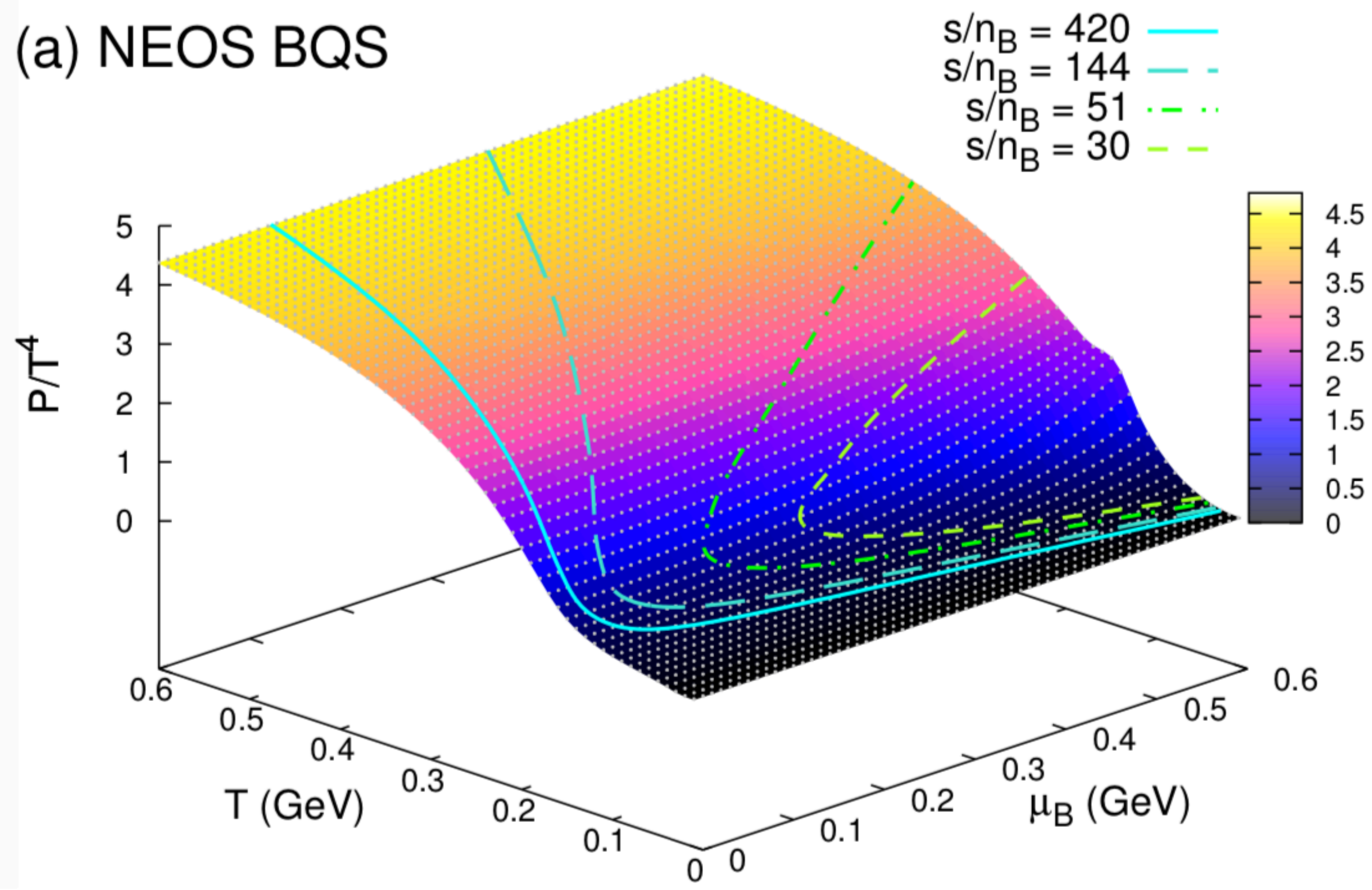

Lattice QCD: Taylor expansion up to the 4th order

$$\frac{P}{T^4} = \frac{P_0}{T^4} + \sum_{l,m,n} \frac{\chi^{B,Q,S}_{l,m,n}}{l!m!n!} \left(\frac{\mu_B}{T}\right)^l \left(\frac{\mu_Q}{T}\right)^m \left(\frac{\mu_S}{T}\right)^n$$

Match to Hadron Resonance Gas model at low T

$$\frac{P}{T^4} = \frac{1}{2}[1 - f(T, \mu_J)] \frac{P_{\rm had}(T, \mu_J)}{T^4} + \frac{1}{2}[1 + f(T, \mu_J)] \frac{P_{\rm lat}(T, \mu_J)}{T^4}$$

$$f(T, \mu_B) = \tanh[(T - T_c(\mu_B)/\Delta T_c]$$

Enabled hydrodynamic simulations at finite μ

THE 3D MC-GLAUBER + STRING MODEL

C. Shen and B. Schenke, Phys.Rev. C97 (2018) 024907

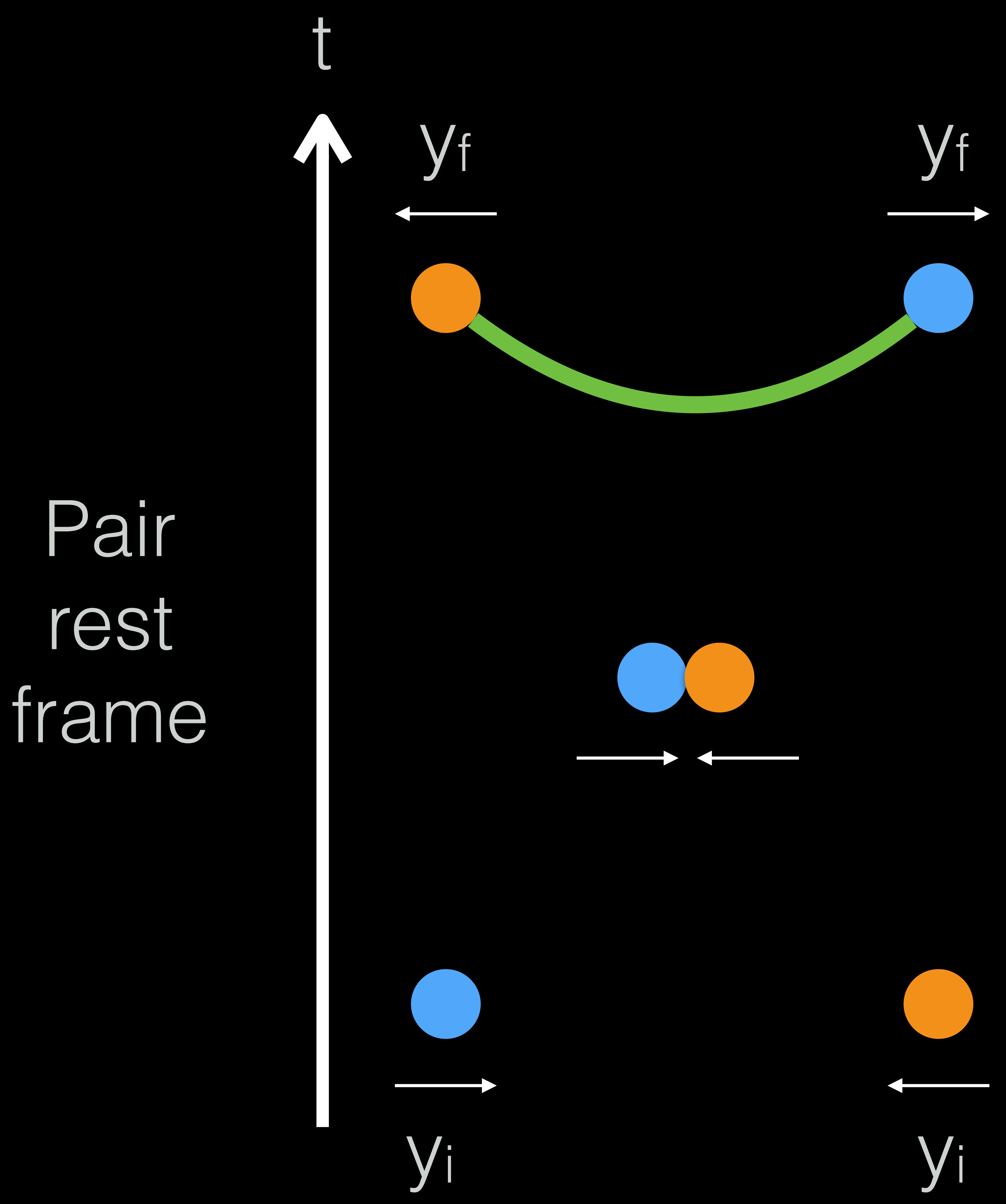

- Collision geometry is determined by MC-Glauber model
- 3 valence quarks are sampled from PDF and randomly picked to lose energy during a collision $\left(\sum_i x_i \leq 1\right)$
- Incoming quarks are decelerated with a classical string tension,

$$dp^\mu = -T^{\mu\nu} d\Sigma_\nu$$

$$T^{\mu\nu} = \begin{pmatrix} \sigma & 0 & 0 & 0 \\ 0 & 0 & 0 & 0 \\ 0 & 0 & 0 & 0 \\ 0 & 0 & 0 & -\sigma \end{pmatrix} \qquad d\Sigma_\nu = (dz, 0, 0, -dt)$$

THE 3D MC-GLAUBER + STRING MODEL

C. Shen and B. Schenke, Phys.Rev. C97 (2018) 024907

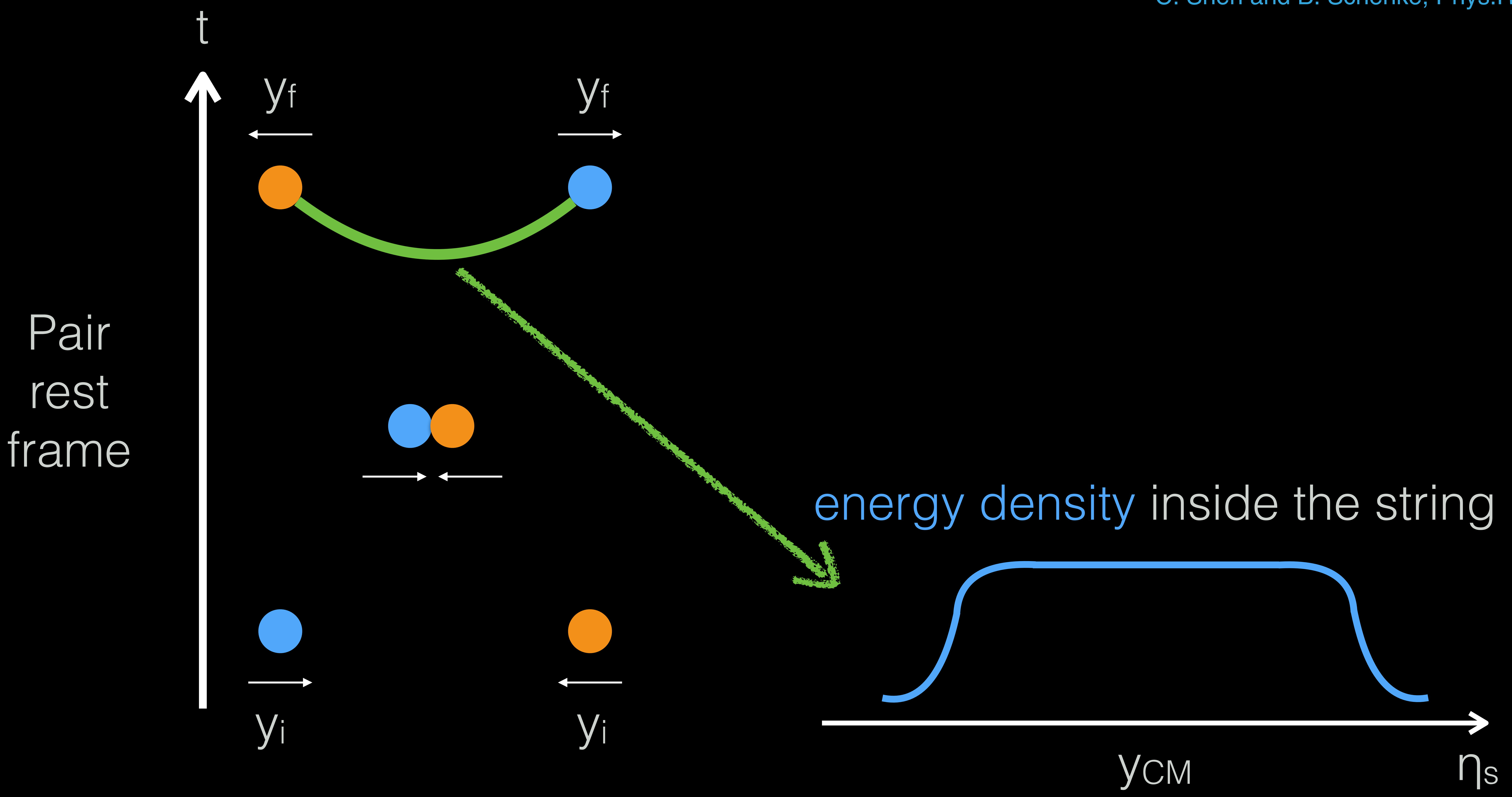

THE 3D MC-GLAUBER + STRING MODEL

C. Shen and B. Schenke, Phys.Rev. C97 (2018) 024907

Pair rest frame

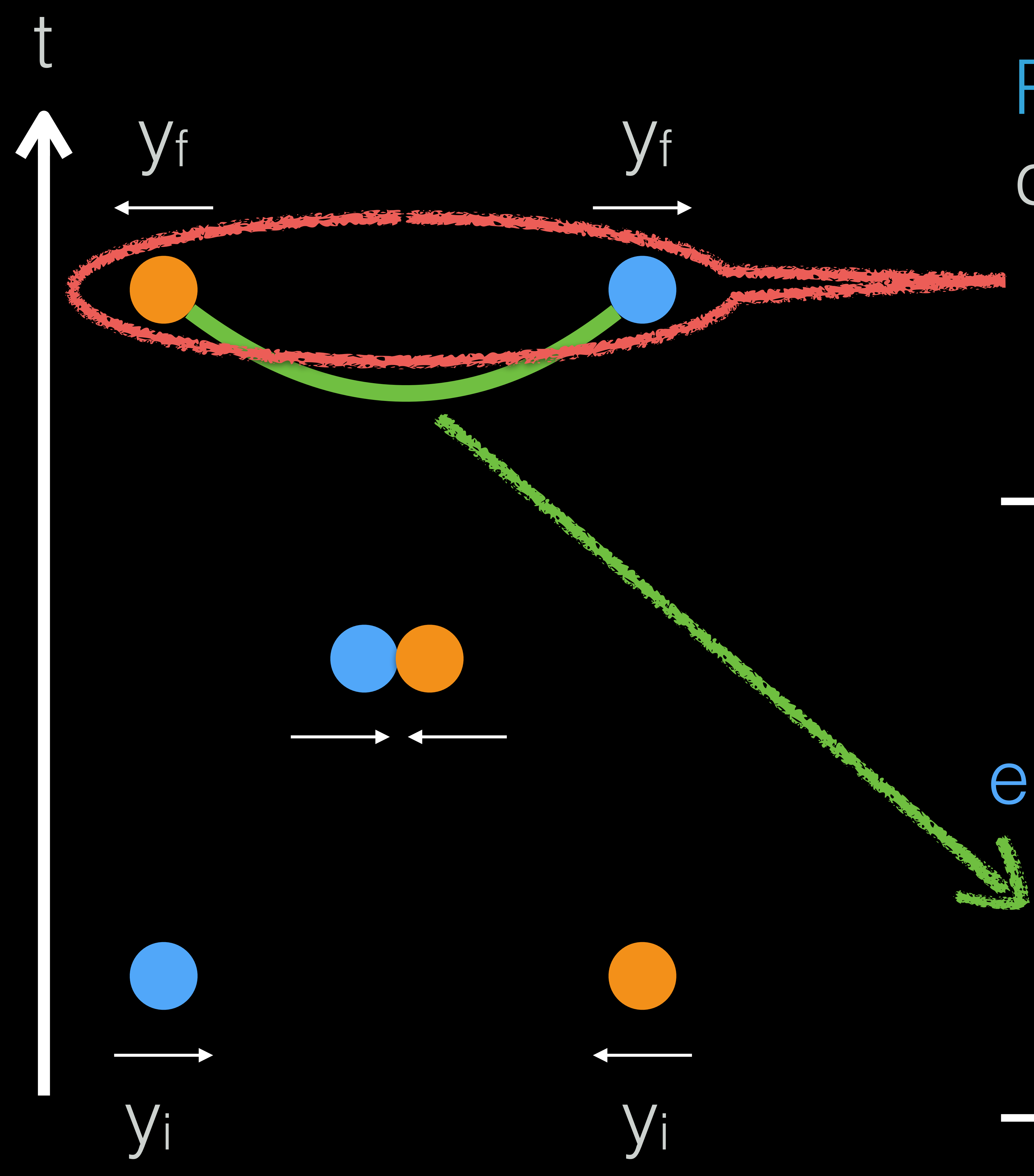

Partons' remaining energy are deposited at the string ends

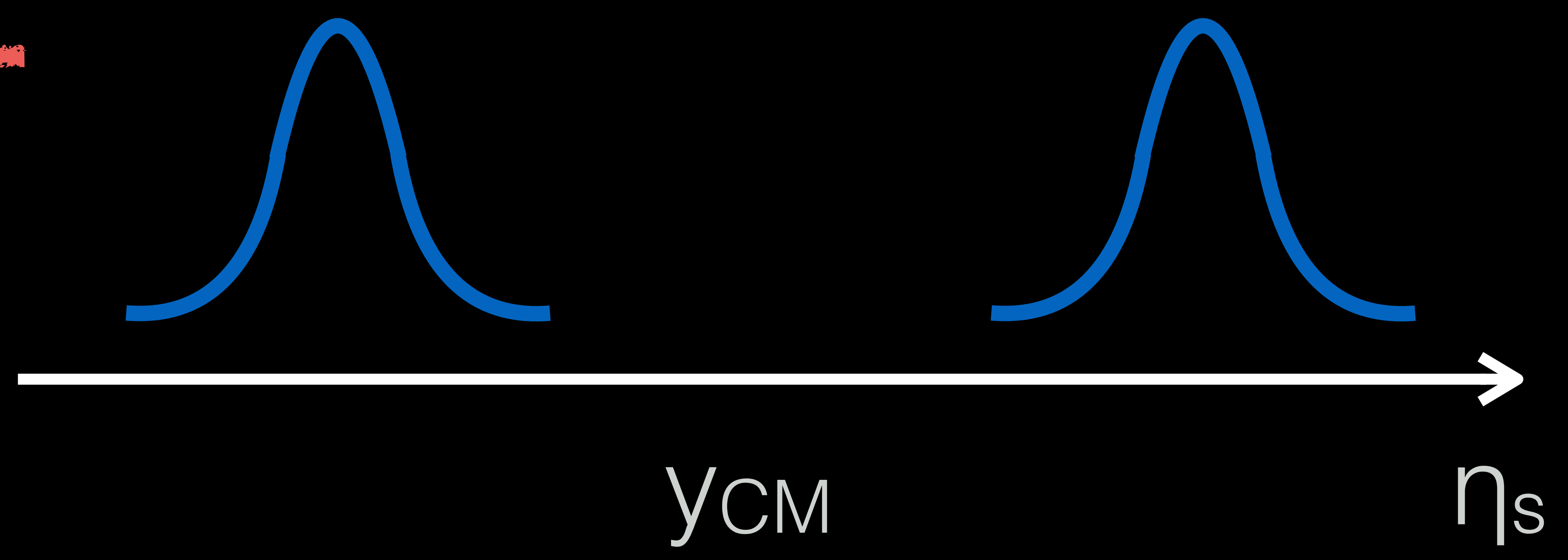

energy density inside the string

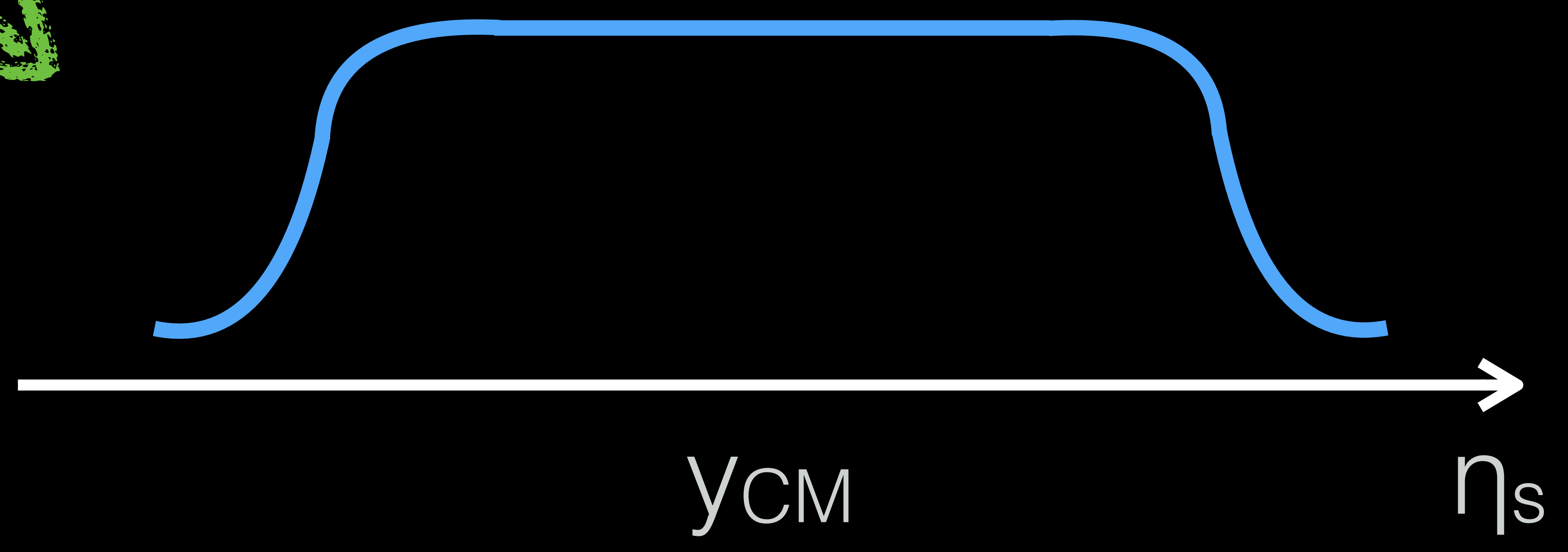

THE 3D MC-GLAUBER + STRING MODEL

C. Shen and B. Schenke, Phys.Rev. C97 (2018) 024907

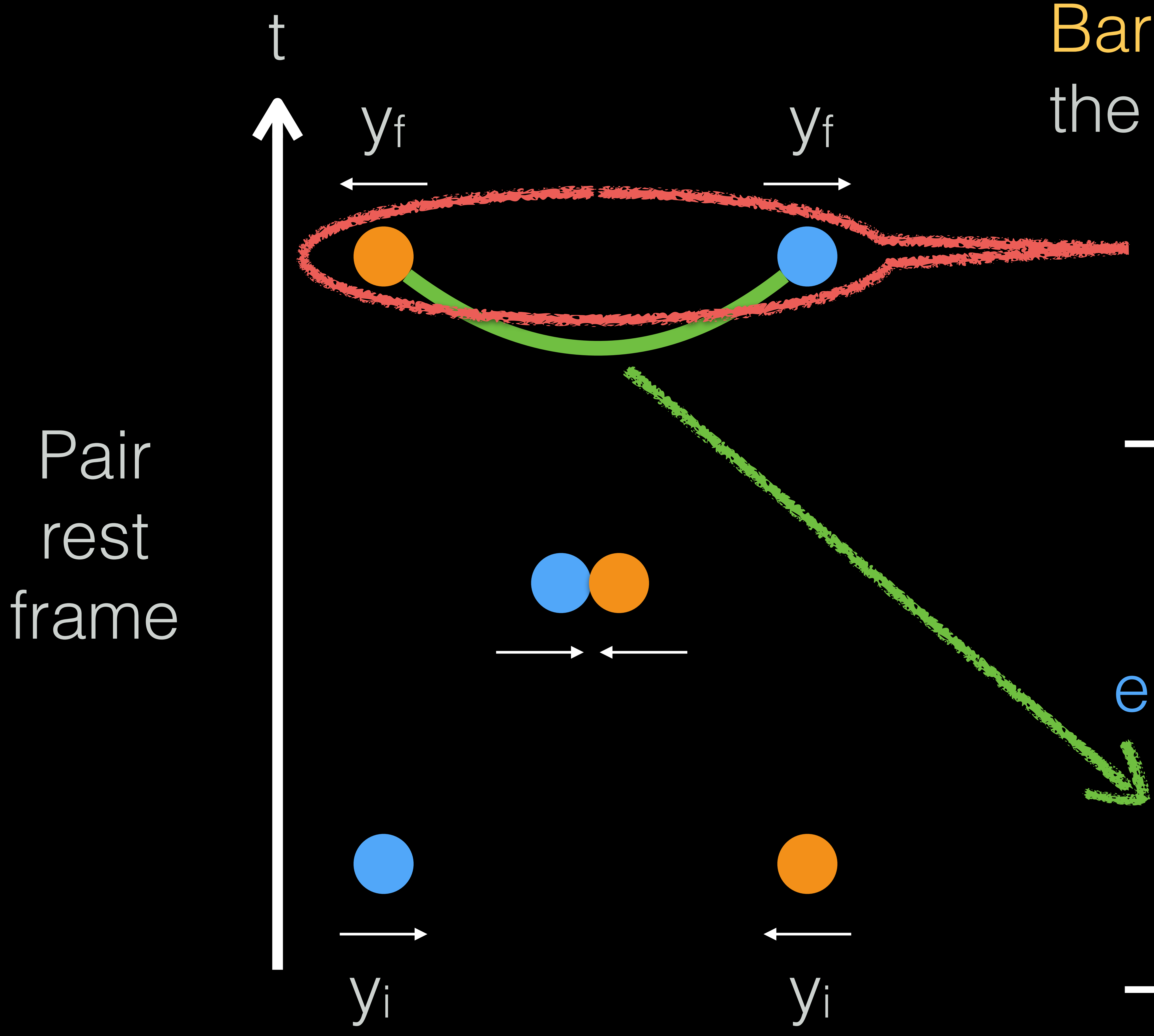

Baryon density are deposited at the string ends or string junctions

D. Kharzeev, Phys. Lett. B 378, 238 (1996)

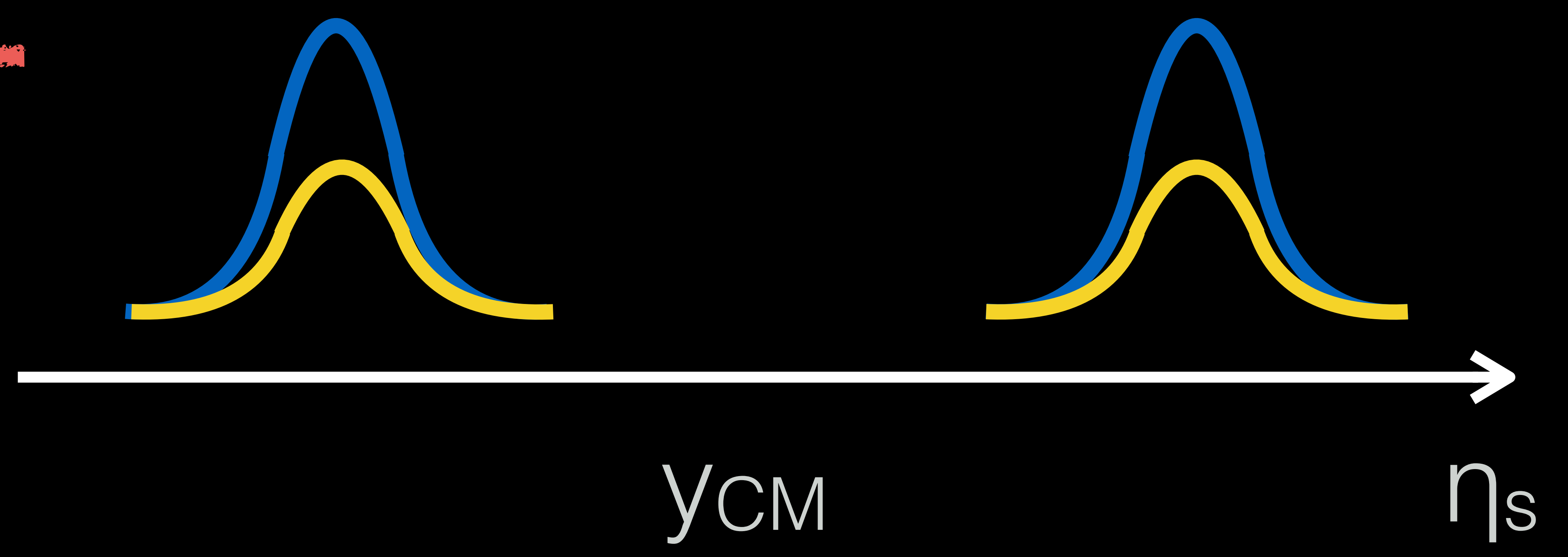

energy density inside the string

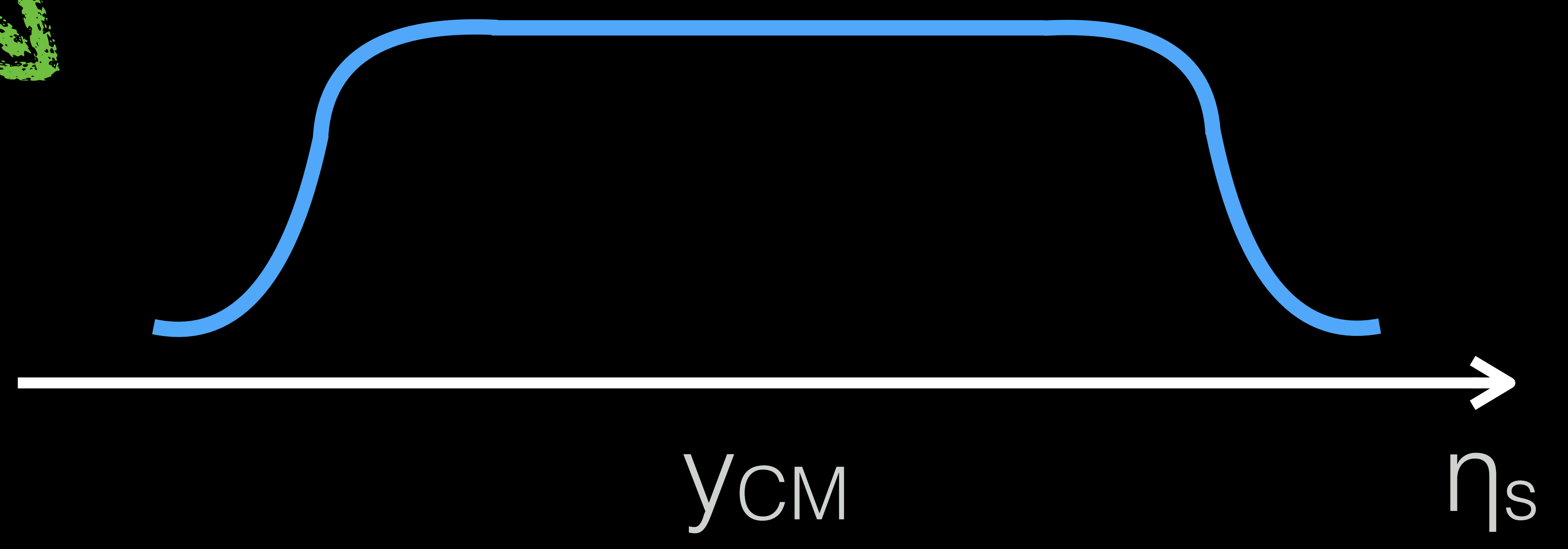

THE 3D MC-GLAUBER + STRING MODEL

C. Shen and B. Schenke, Phys.Rev. C97 (2018) 024907

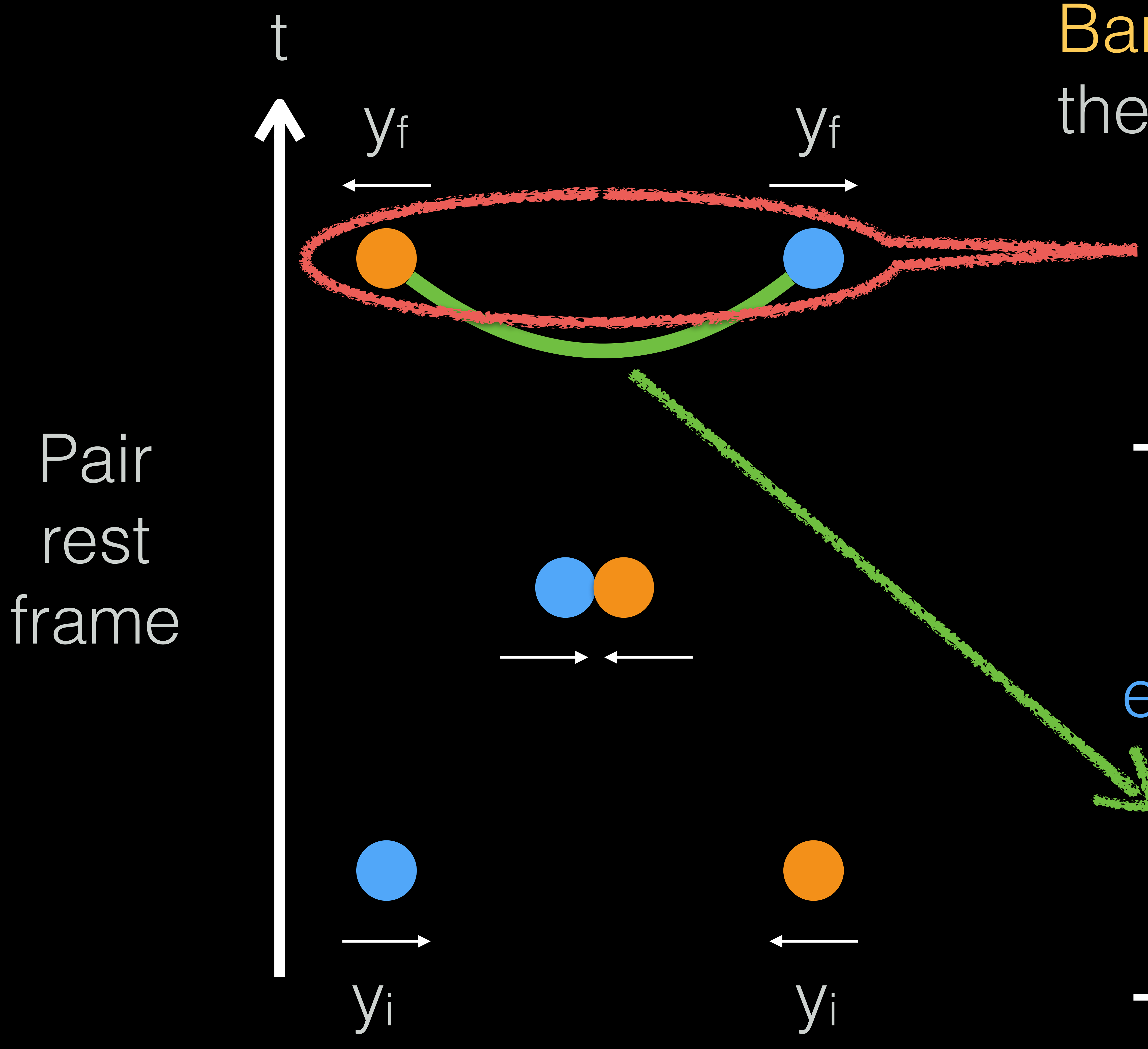

Baryon density are deposited at the string ends or string junctions

D. Kharzeev, Phys. Lett. B 378, 238 (1996)

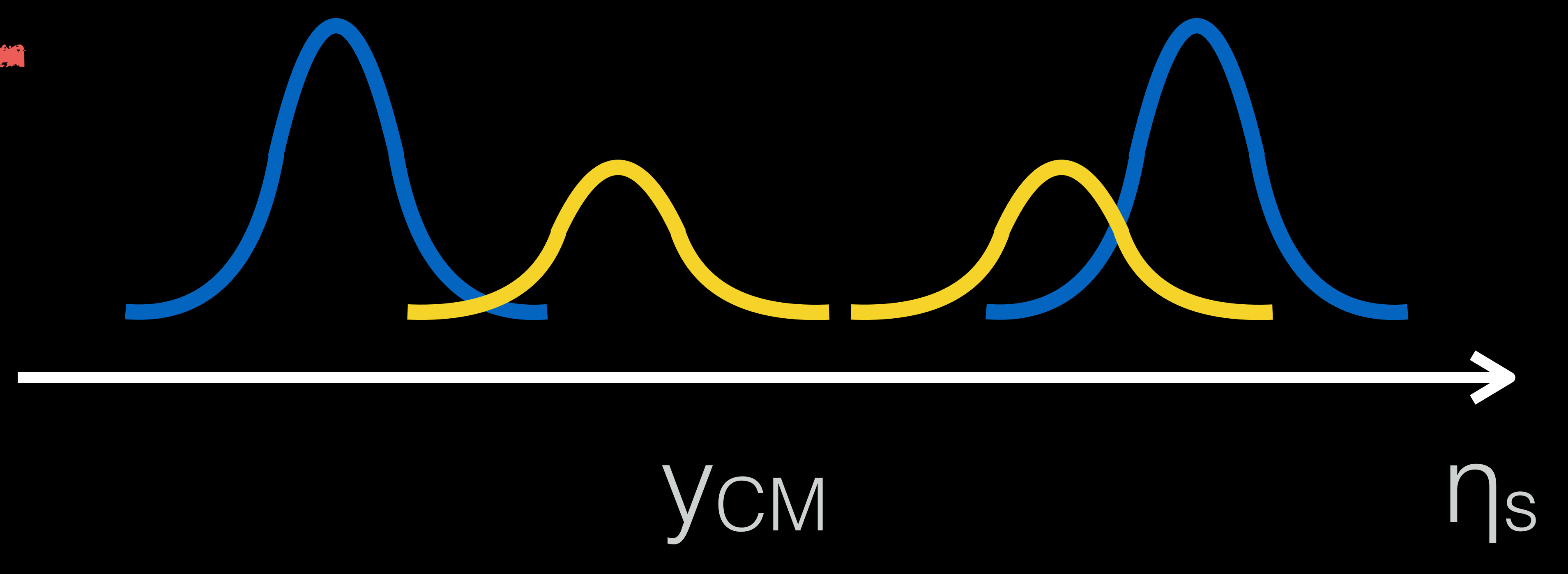

energy density inside the string

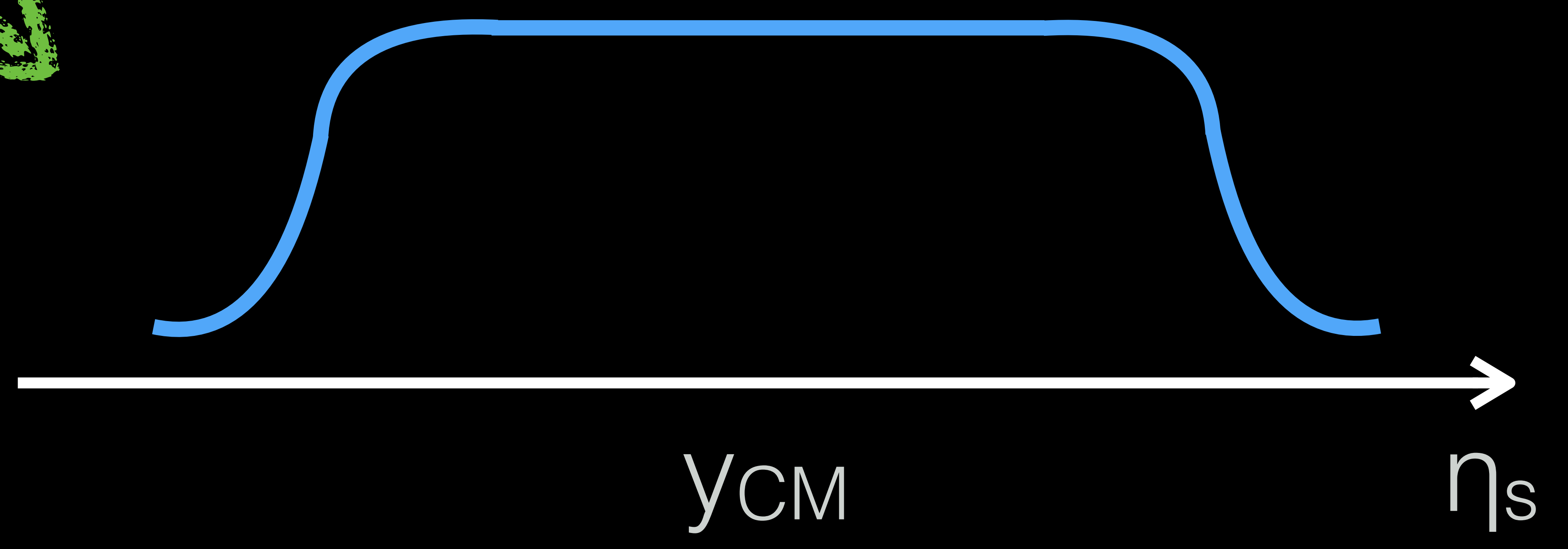

THE 3D MC-GLAUBER + STRING MODEL

C. Shen and B. Schenke, Phys.Rev. C97 (2018) 024907

Pair rest frame

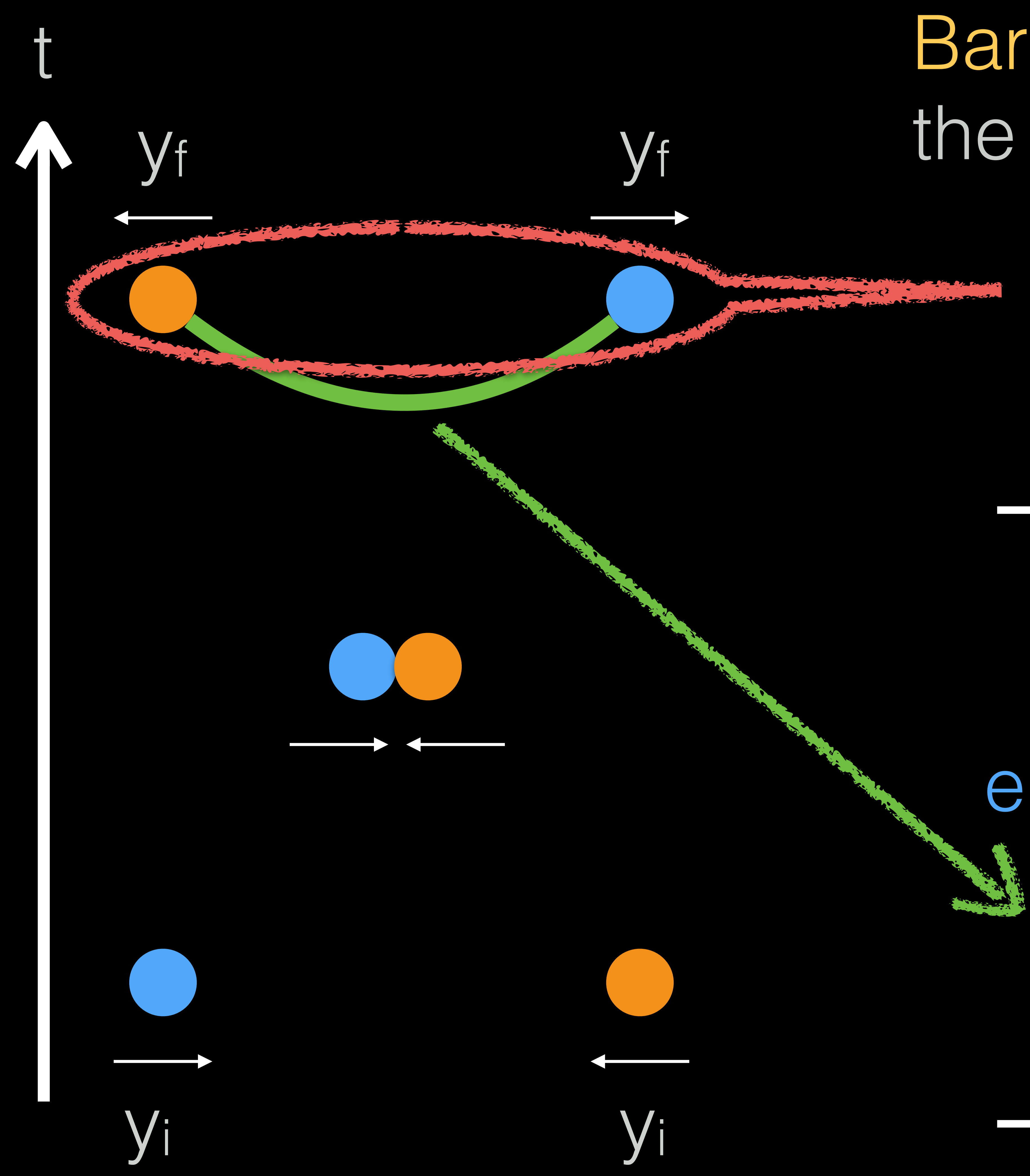

Baryon density are deposited at the string ends or string junctions

D. Kharzeev, Phys. Lett. B 378, 238 (1996)

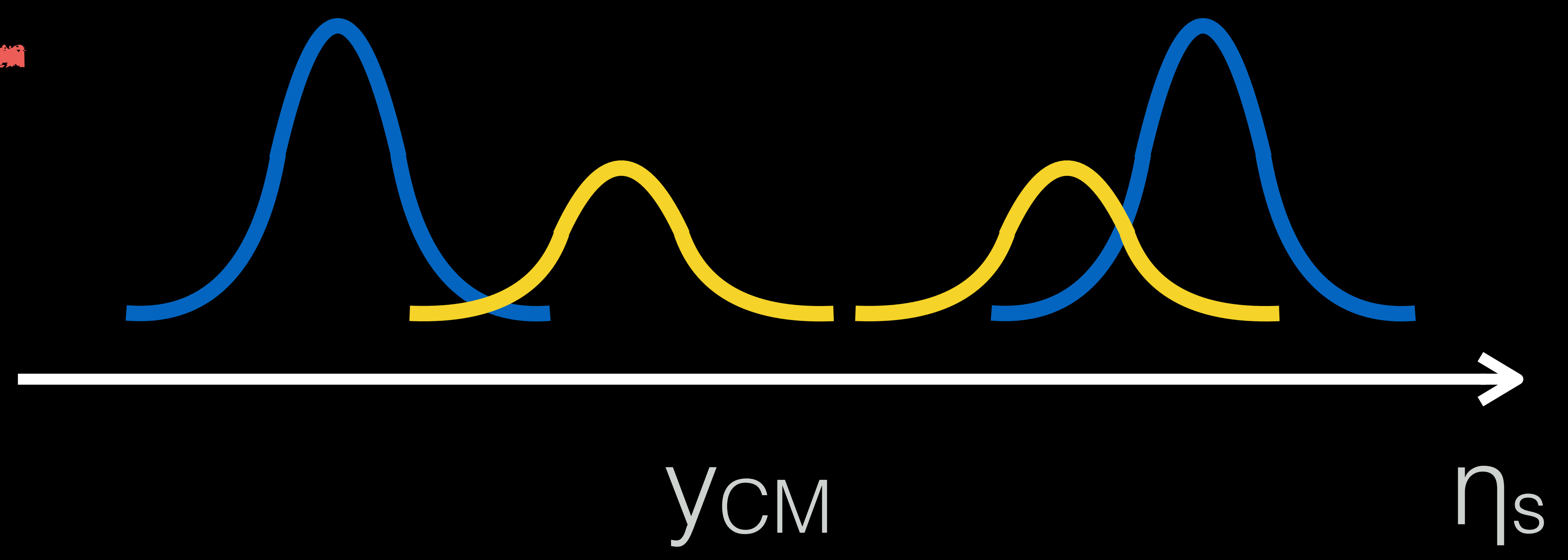

energy density inside the string

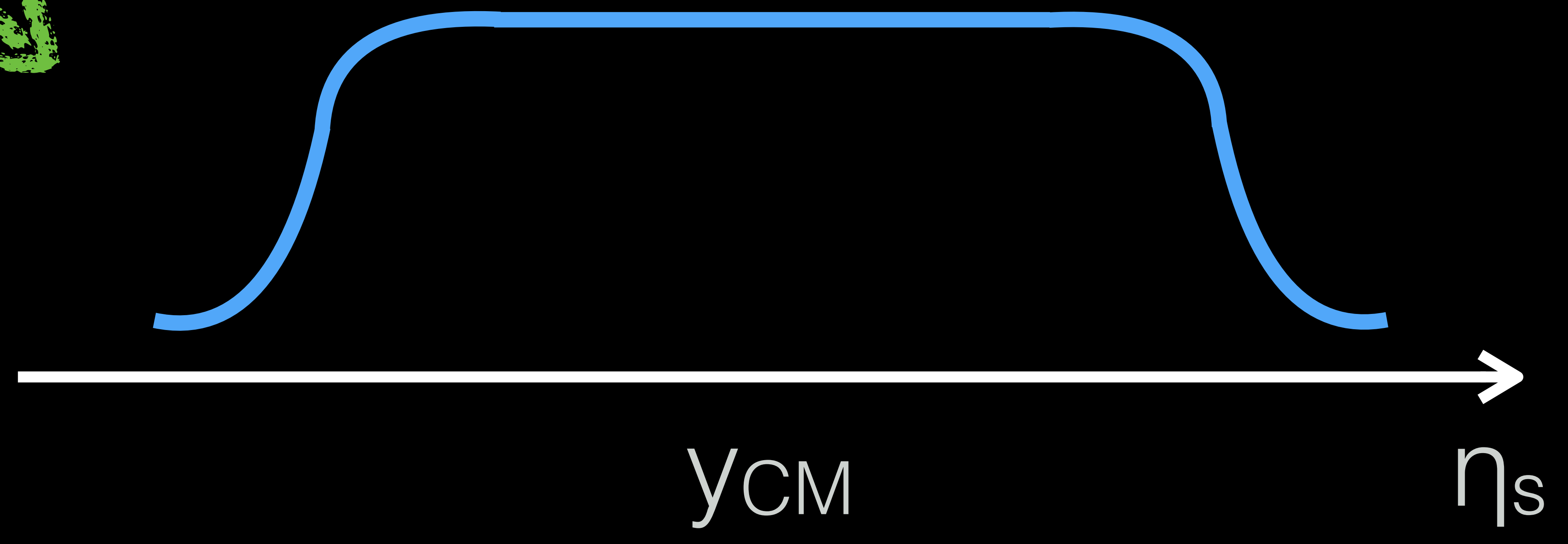

Imposed conservation for energy, momentum, and net baryon density

PARTICLE PRODUCTION AT THE RHIC BES

B. Schenke and C. Shen, in preparation

Parameterize the valence quark energy loss

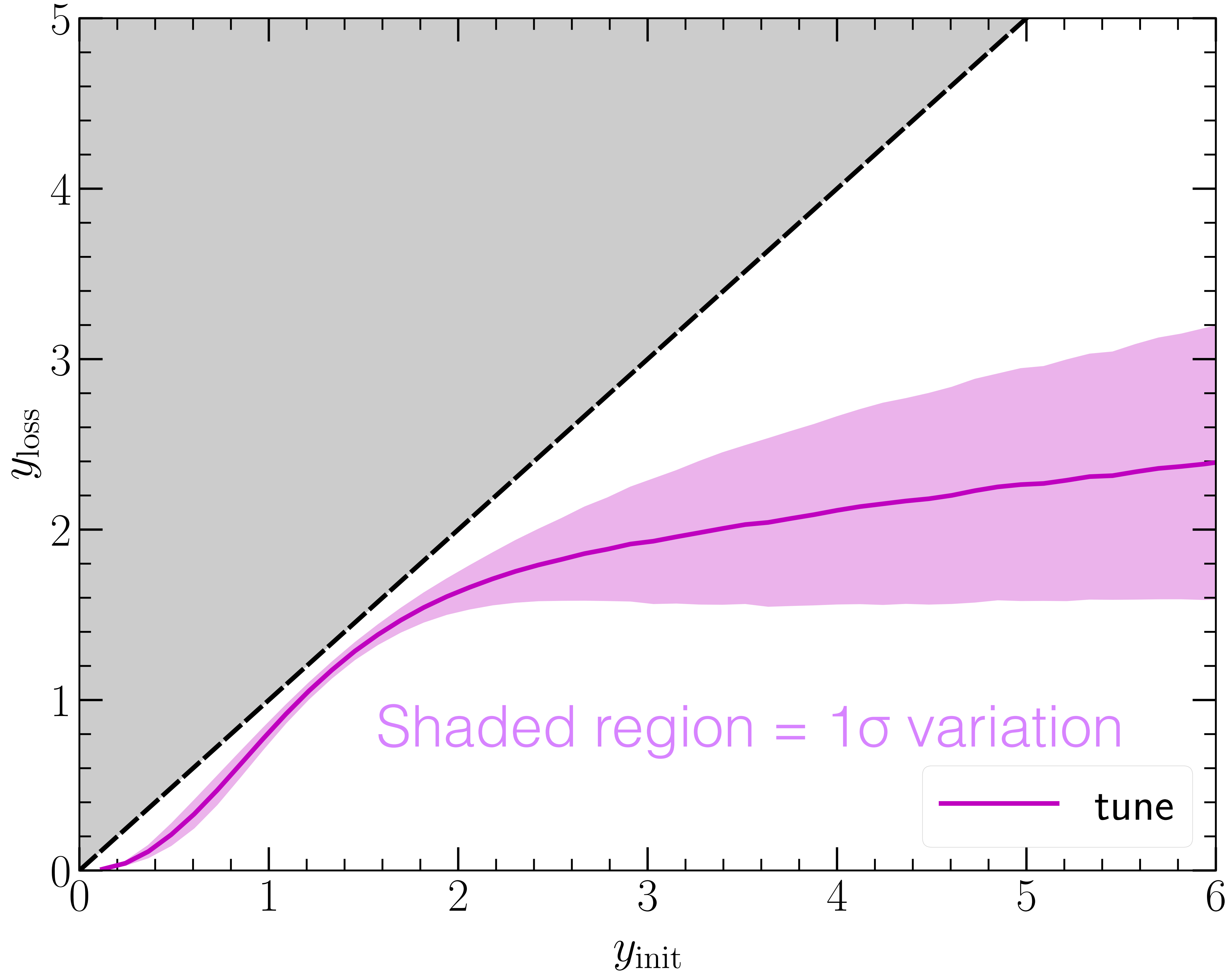

$$\langle y_{\rm loss} \rangle = A y_{\rm init}^{\alpha_2} [\tanh(y_{\rm init})]^{\alpha_1 - \alpha_2}$$

- A: the slope
- At small y: $\langle y_{\rm loss} \rangle \propto y_{\rm init}^{\alpha_1}$
- At large y: $\langle y_{\rm loss} \rangle \propto y_{\rm init}^{\alpha_2}$
- Std of $y_{\rm loss}$ fluctuations: σ_y ($y_{\rm loss} \in [0, y_{\rm init}]$)

PARTICLE PRODUCTION AT THE RHIC BES

B. Schenke and C. Shen, in preparation

- Calibrated with minimum bias pp measurements at mid-rapidity and their multiplicity distribution
- The discrepancy at the forward rapidity can be improved by fine tuning of the beam remnant dynamics

EXTEND 3D DESCRIPTION TO SMALL SYSTEMS AT BES

B. Schenke and C. Shen, in preparation

- Our model reproduces the STAR multiplicity distribution in the d+Au collisions at 200 GeV
- The predicted charged hadron rapidity distribution agrees well with the PHENIX measurements from central to peripheral collisions
- The role of spectators in the forward rapidity need further investigation at low energies

PARTICLE PRODUCTION AT THE RHIC BES

B. Schenke and C. Shen, in preparation

Parameterize the valence quark energy loss

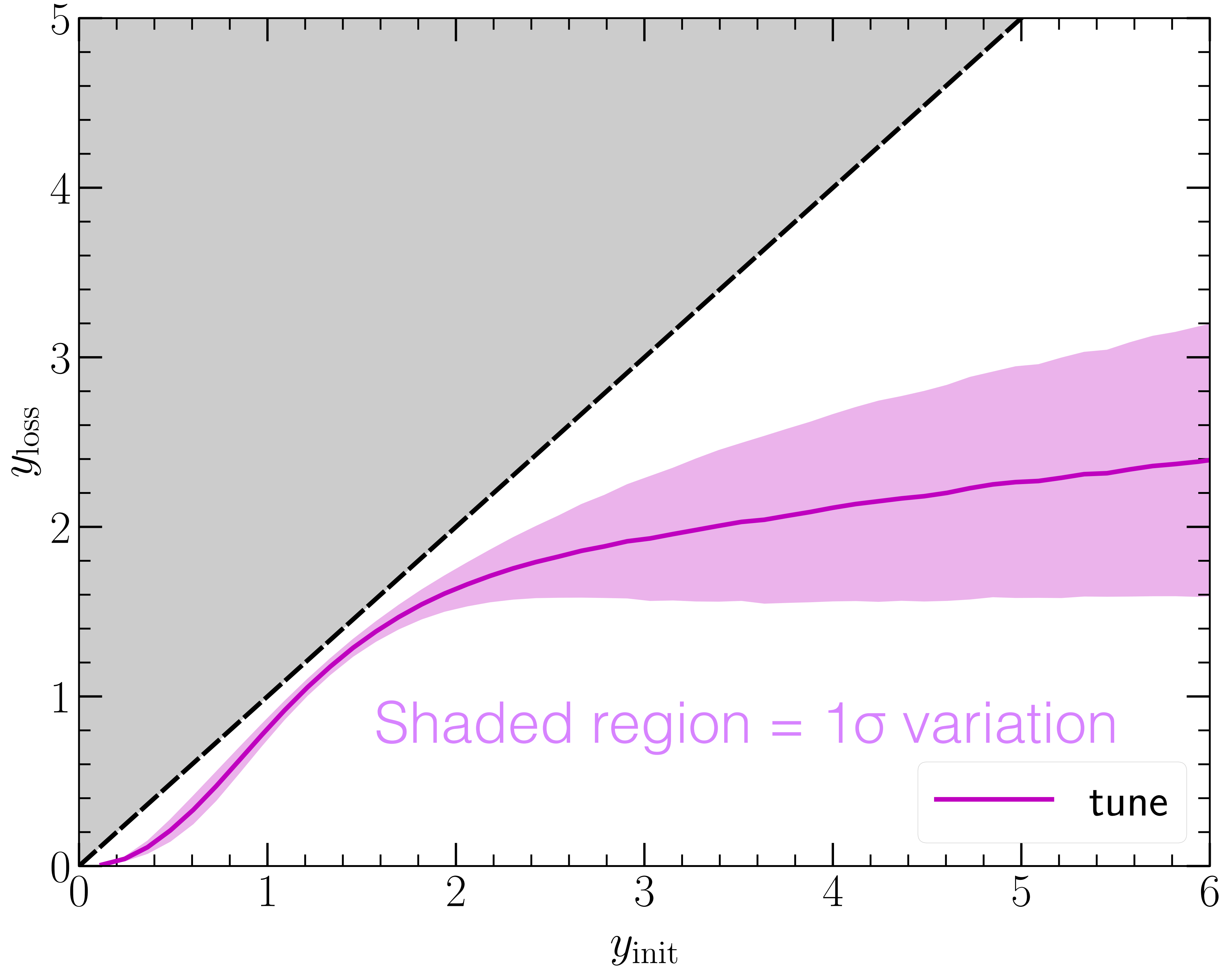

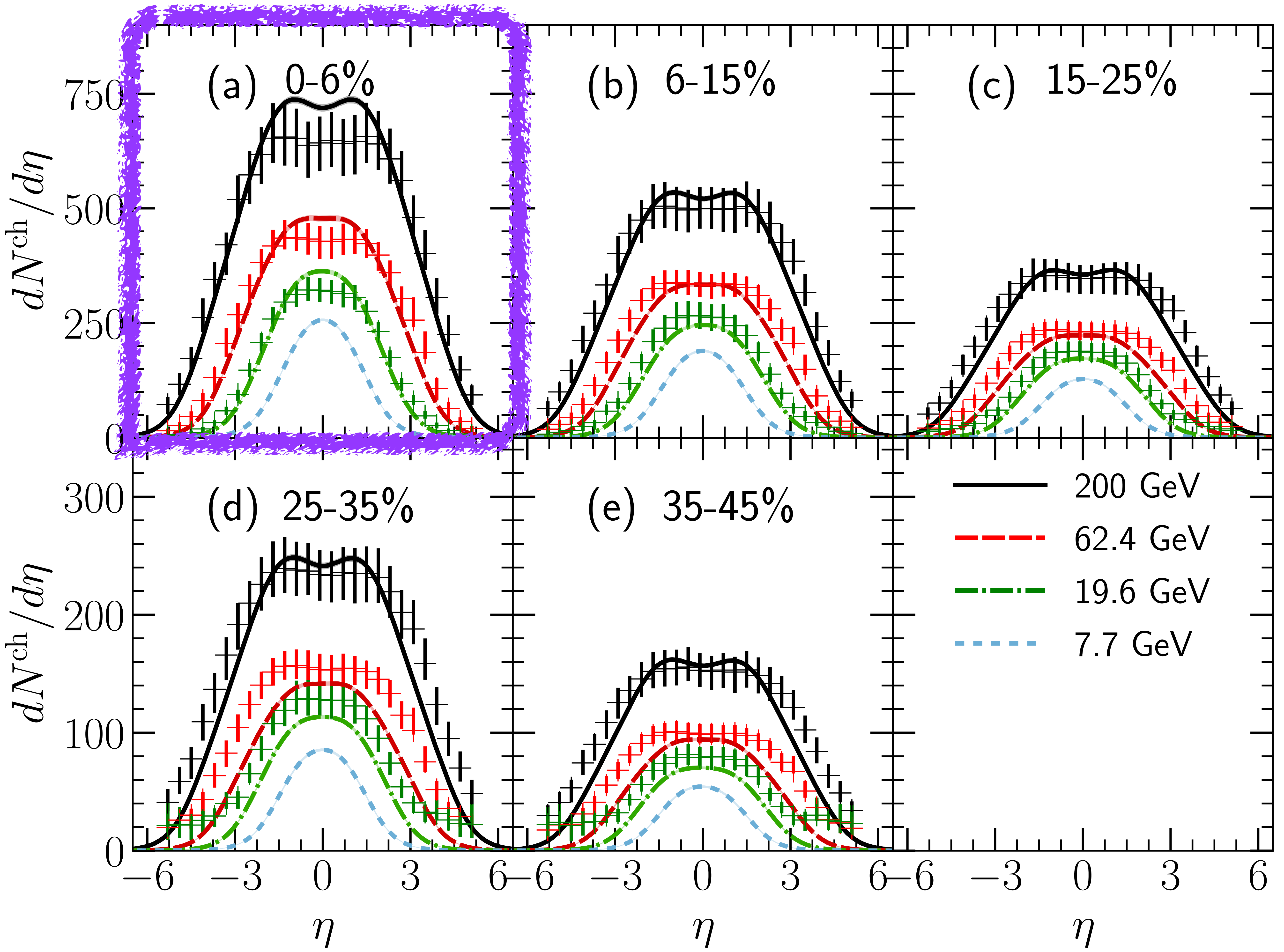

- Further adjust a coherent parameter in central AA collisions

PARTICLE PRODUCTION AT THE RHIC BES

B. Schenke and C. Shen, in preparation

Parameterize the valence quark energy loss

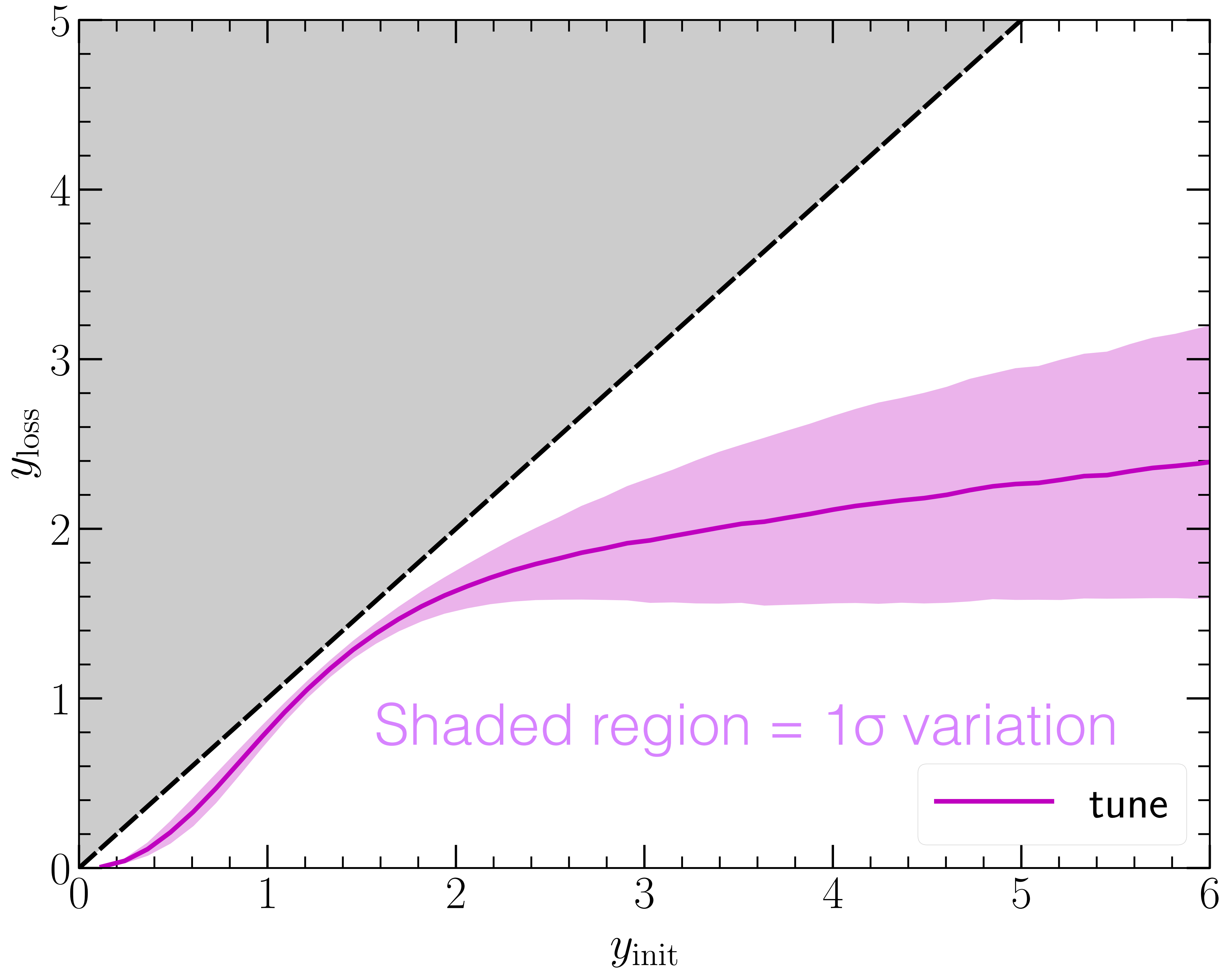

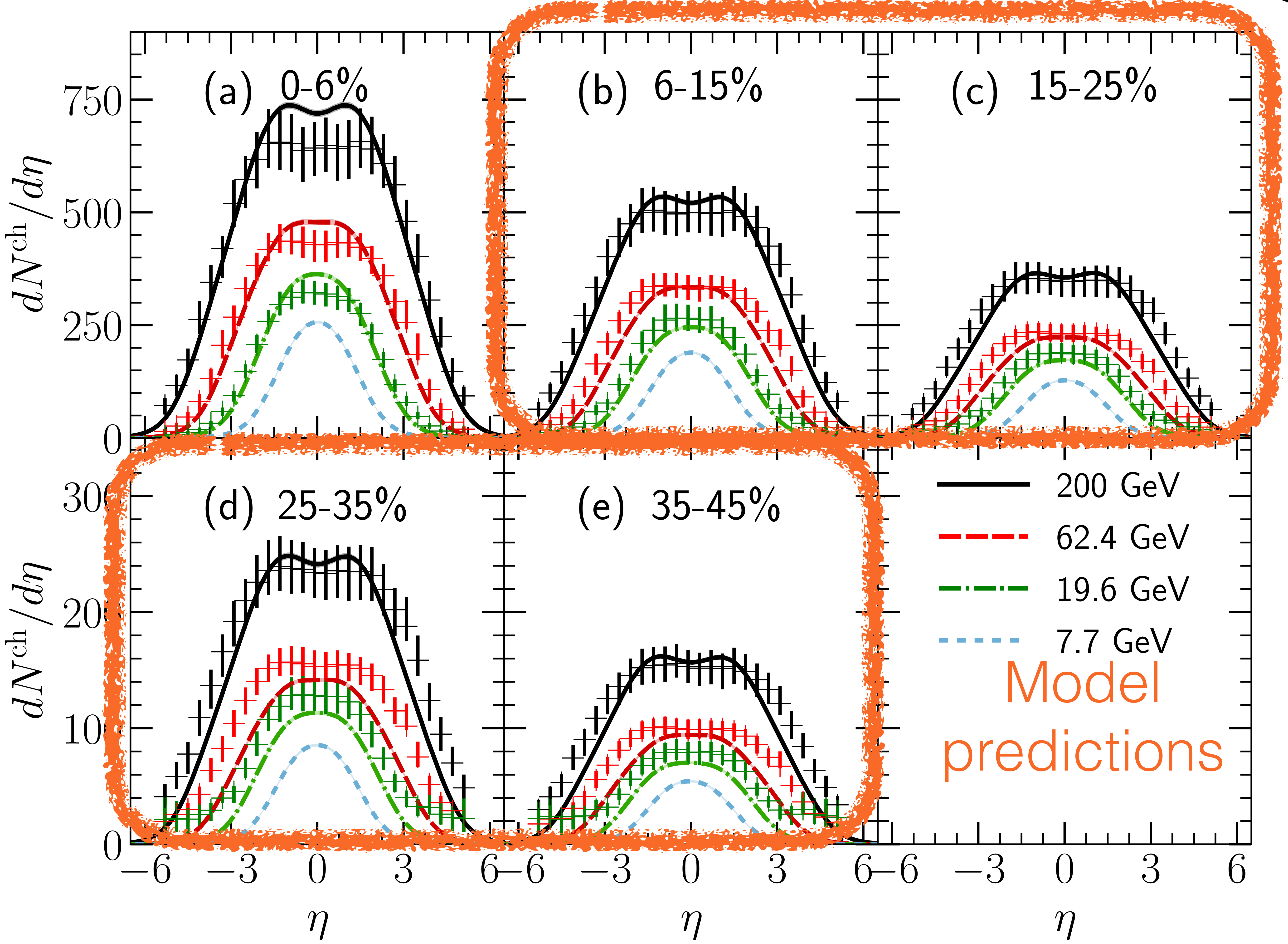

- A good description of particle production for all centrality bins

INITIAL STATE BARYON STOPPING

C. Shen and B. Schenke, in preparation

- Allowing the initial baryon charges to fluctuate to string junctions provides a consistent description of net proton rapidity distribution from 7.7 to 200 GeV

D. Kharzeev, Phys. Lett. B 378, 238 (1996)

Quantify the early-stage baryon stopping at RHIC

CENTRALITY AND RAPIDITY DEPENDENCE OF NET PROTONS

B. Schenke and C. Shen, in preparation

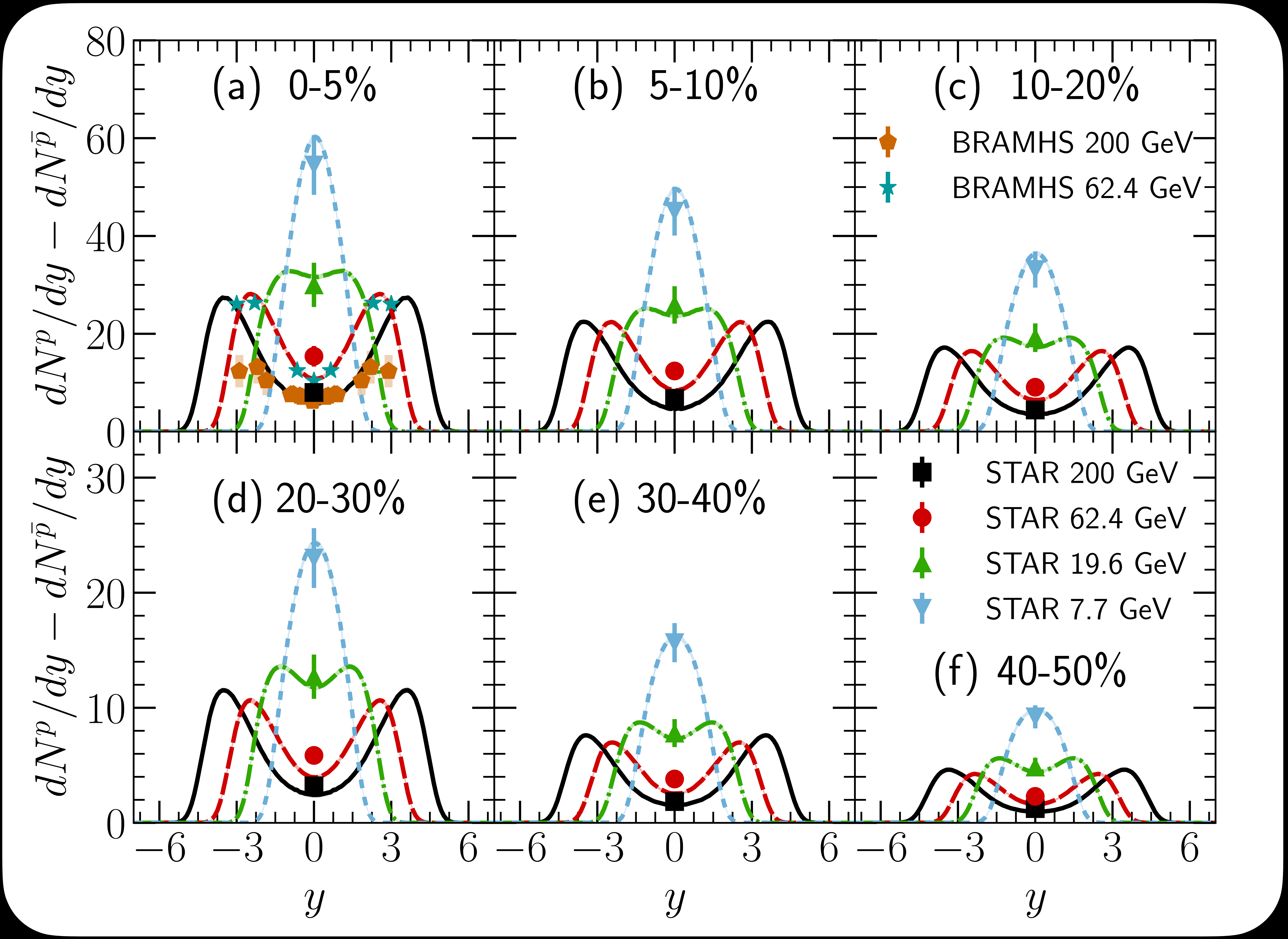

- Predictions for the net proton rapidity and centrality dependence at RHIC BES energies
- Our results at mid-rapidity are consistent with the STAR measurements
- Measurements of the rapidity dependence can further constrain the distributions of initial baryon charges

AVERAGE TRANSVERSE MOMENTUM AT RHIC BES

B. Schenke and C. Shen, in preparation

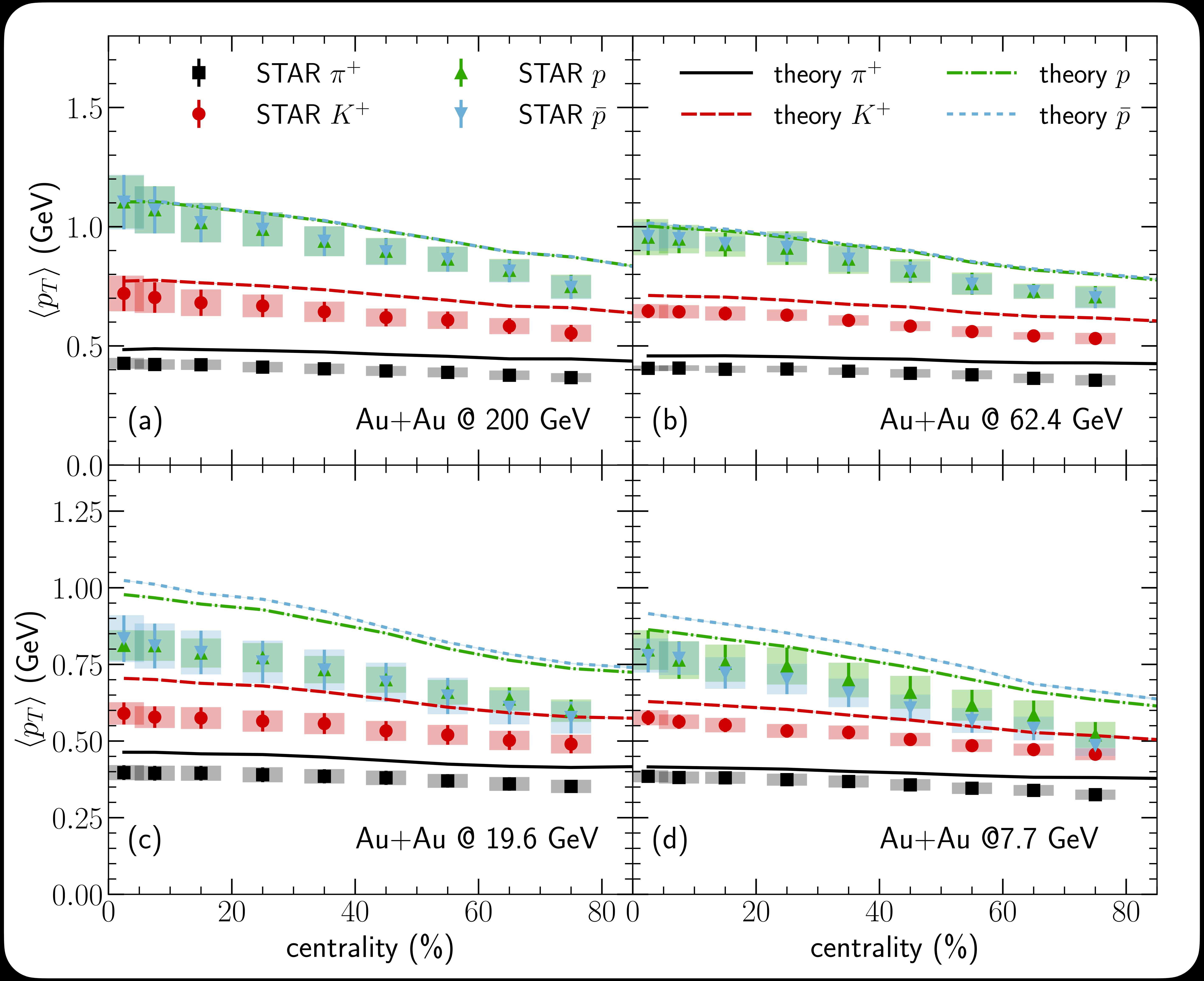

- The averaged transverse momenta of identified particles are slightly overestimated, which suggests the need of a non-zero but small bulk viscosity

FLOW ANISOTROPY AT RHIC BES

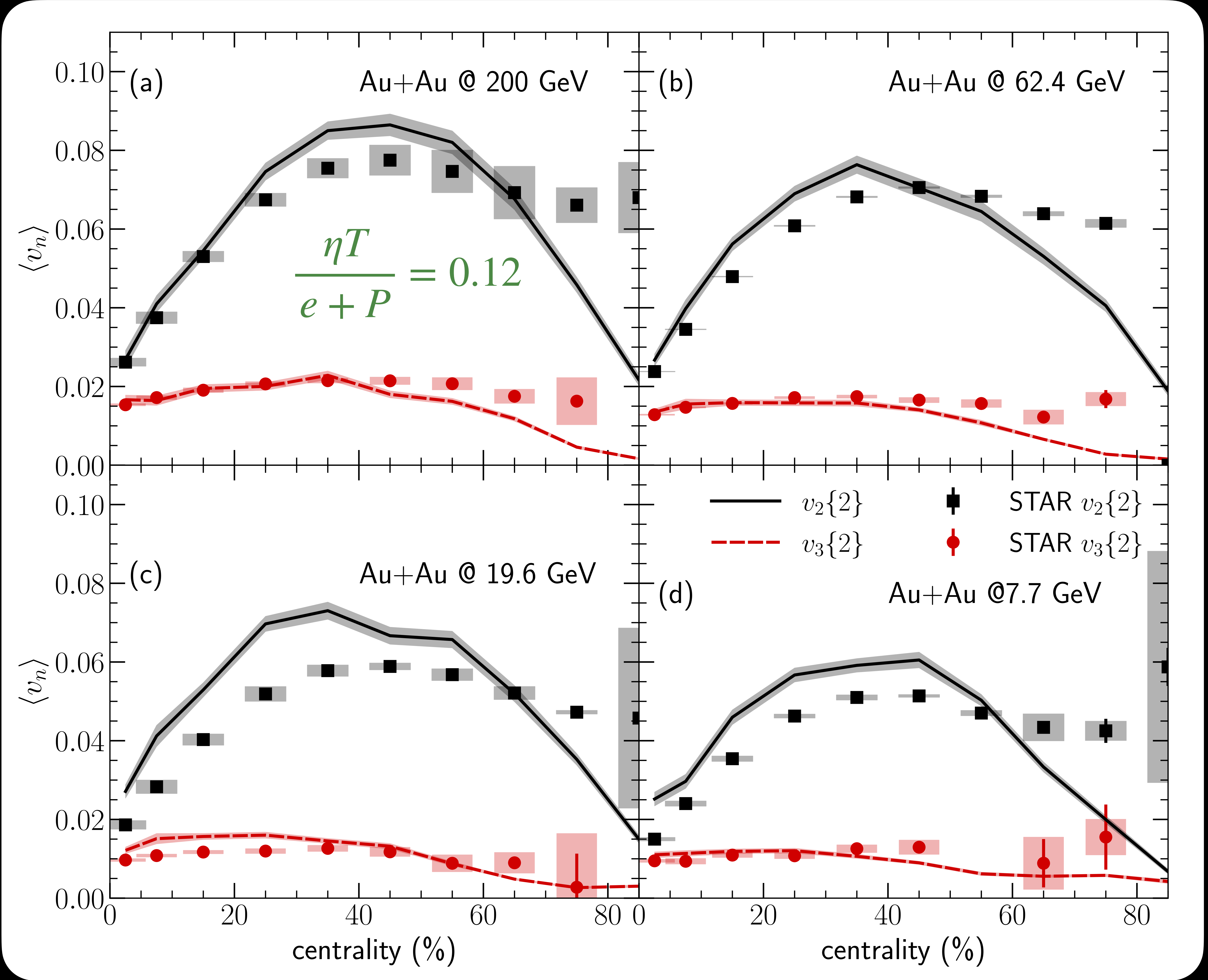

B. Schenke and C. Shen, in preparation

- With limited statistics, we compare the anisotropic flow coefficients with STAR at different collision energies
- As the collision energy decreases, the theory starts to overestimate v_2 suggesting the QGP $\eta/s(T, \mu_B)$ grows at low T and large μ_B

SLOWING DOWN NEAR THE QCD CRITICAL POINT

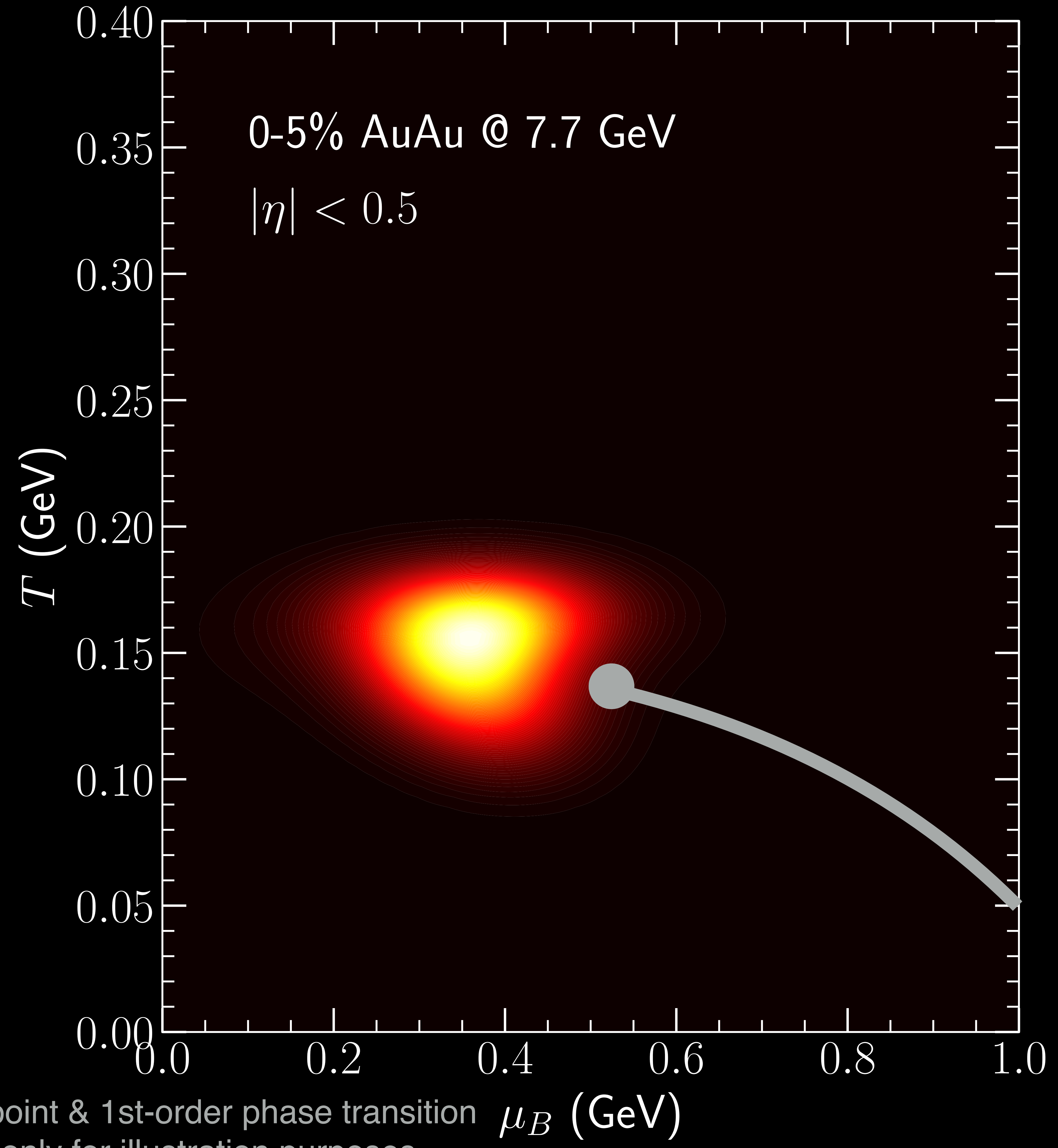

critical point & 1st-order phase transition line are only for illustration purposes

Thomas Vojta, AIP Conf. Proc. 1550, 188 (2013)

$T > T_c$

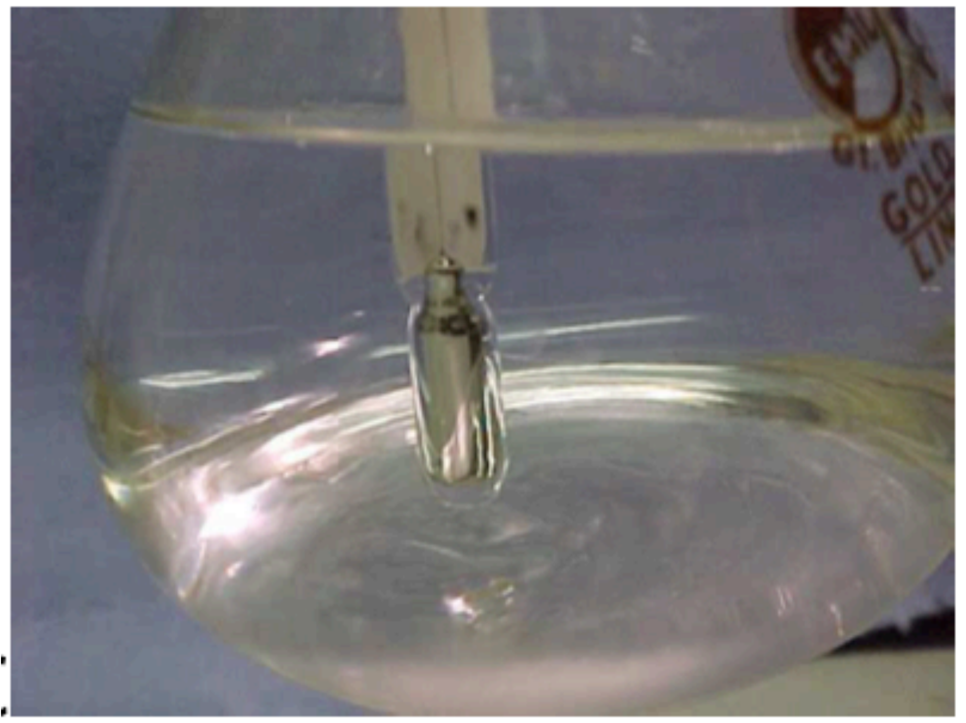

$T \sim T_c$

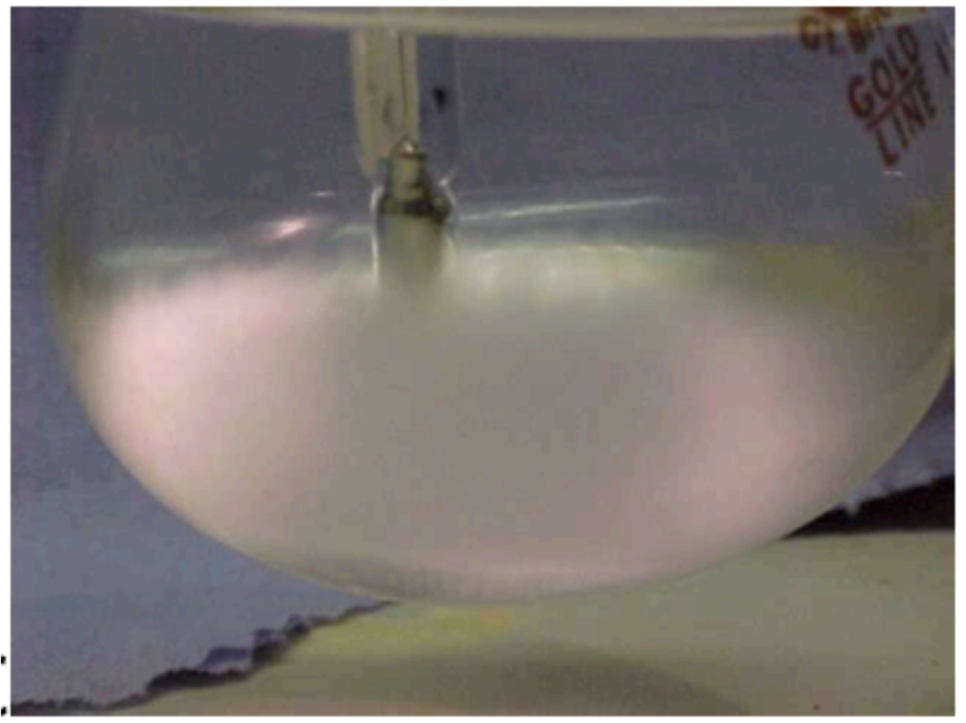

$T < T_c$

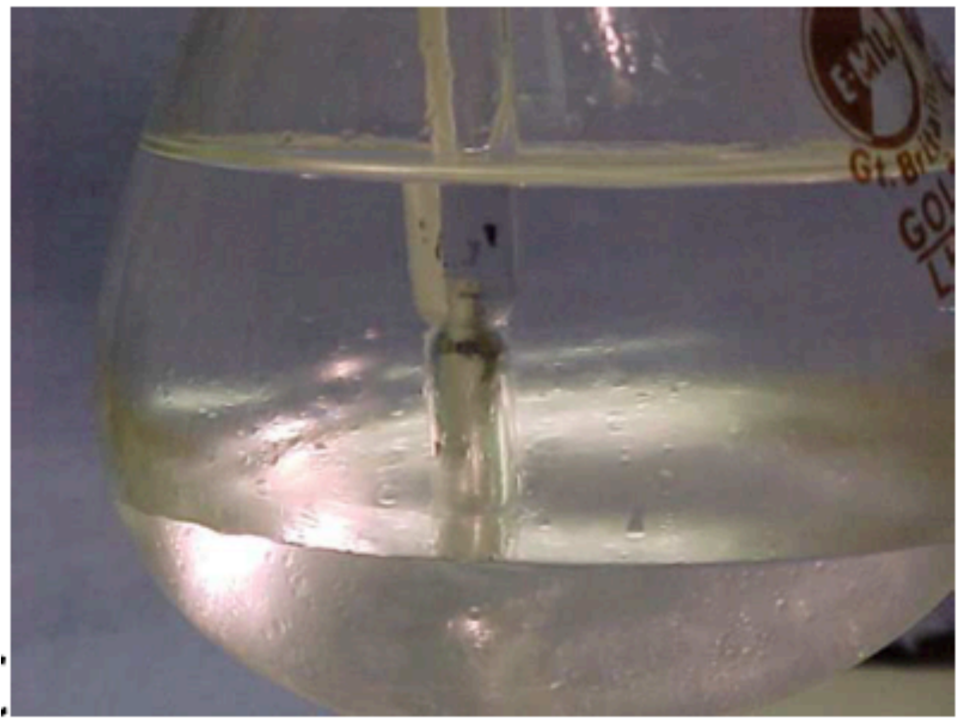

BUILDING CRITICALITY IN QCD EOS

J. Noronha-Hostler, P. Parotto, C. Ratti and J. M. Stafford, Phys. Rev. C100, 064910 (2019)
J. M. Stafford *et. al*, arXiv:2103.08146 [hep-ph]

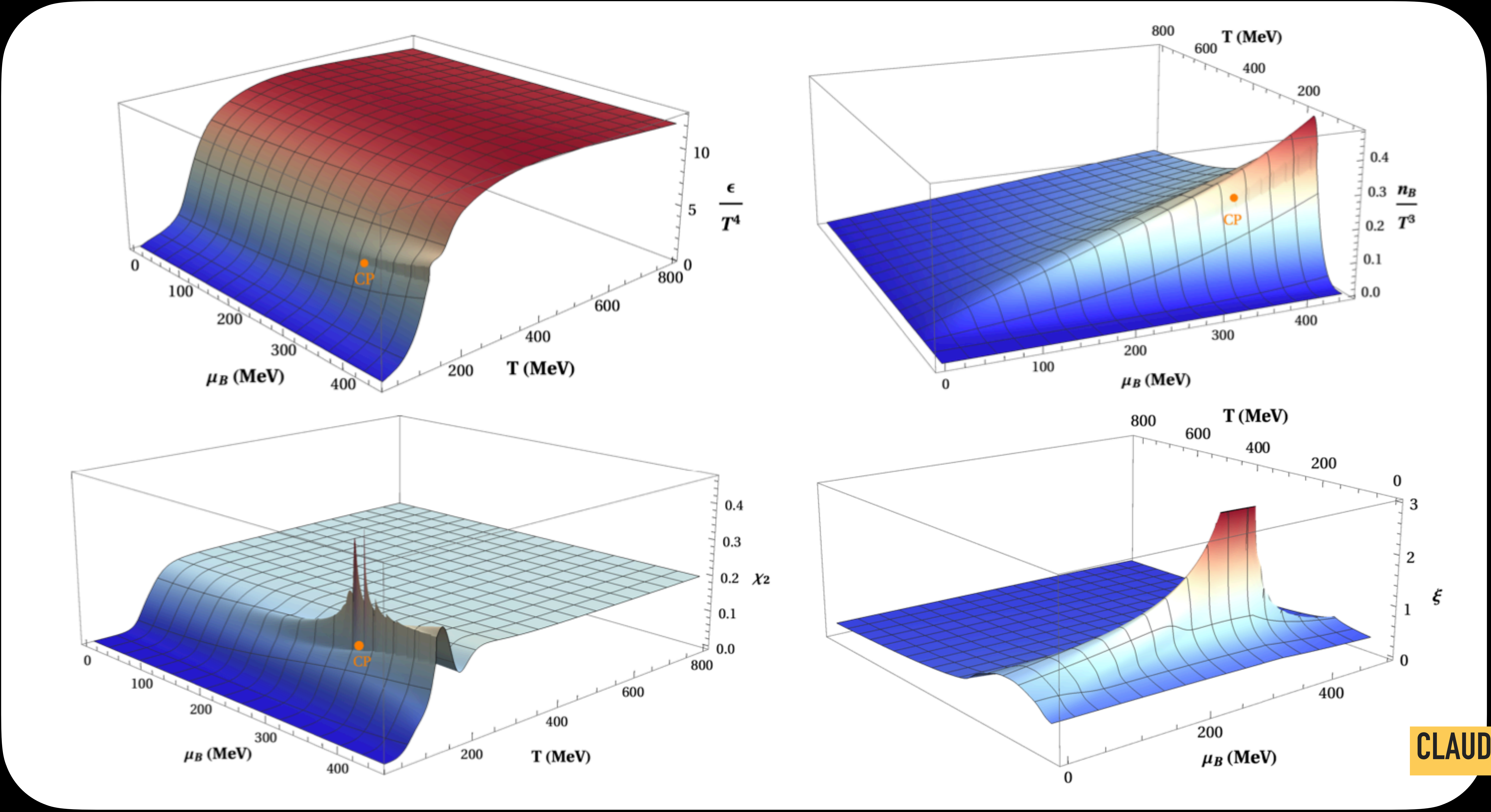

CLAUDIA RATTI 13:50

NON-EQUILIBRIUM DYNAMICS OF CRITICAL FLUCTUATIONS

- Stochastic approach

Kapusta, Muller, Stephanov, '12; Young '14; Singh *et al.* '18; Nahrgang *et al.* '19; …

$$\partial_t \tilde{\psi} = -\nabla \cdot (J[\tilde{\psi}] + \xi)$$

stochastic variable

noise

conserved quantity:
$\psi = \langle \tilde{\psi} \rangle = (T^{00}, T^{0j}, J^0)$
flux: $J = (T^{i0}, T^{ij}, J^i)$

- Deterministic approach $G = \langle \tilde{\psi}\tilde{\psi} \rangle - \langle \tilde{\psi} \rangle \langle \tilde{\psi} \rangle$

$$\partial_t \psi = -\nabla \cdot J[\psi, G]$$

$$\partial_t G = -\Gamma(G - G^{\mathrm{eq}}[\psi]) + \mathscr{F}[\mathscr{G}]$$

Relaxation

background gradients

Andreev '78; Akamatsu *et al.* '16, '18; Matinez, Schaefer '18; An *et al.*, '19-'20; …

NON-EQUILIBRIUM DYNAMICS OF CRITICAL FLUCTUATIONS

- Stochastic approach
- Deterministic approach

M. Nahrgang *et al.*, Phys. Rev. D99, 116015 (2019)

equilibrium

Bjorken medium

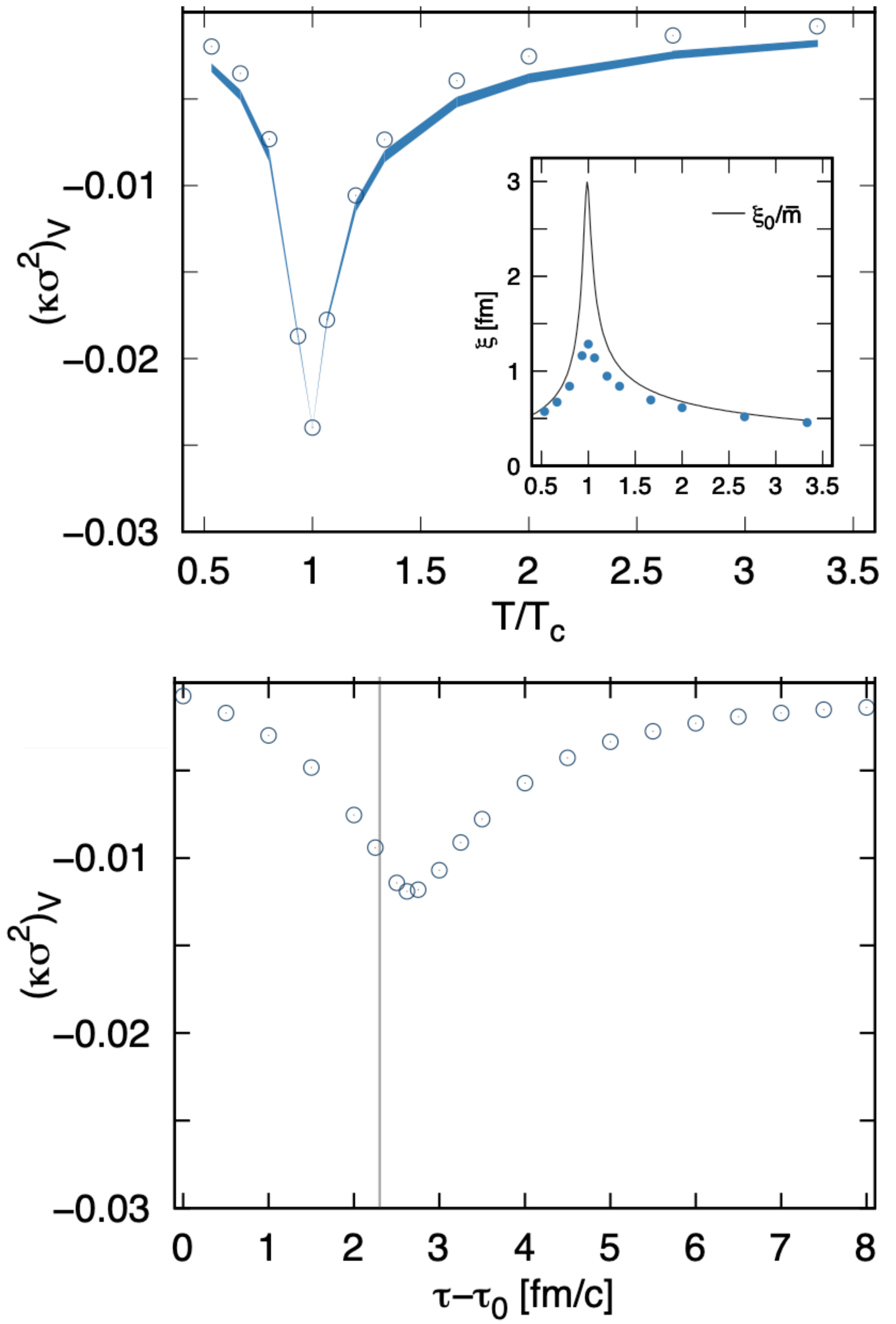

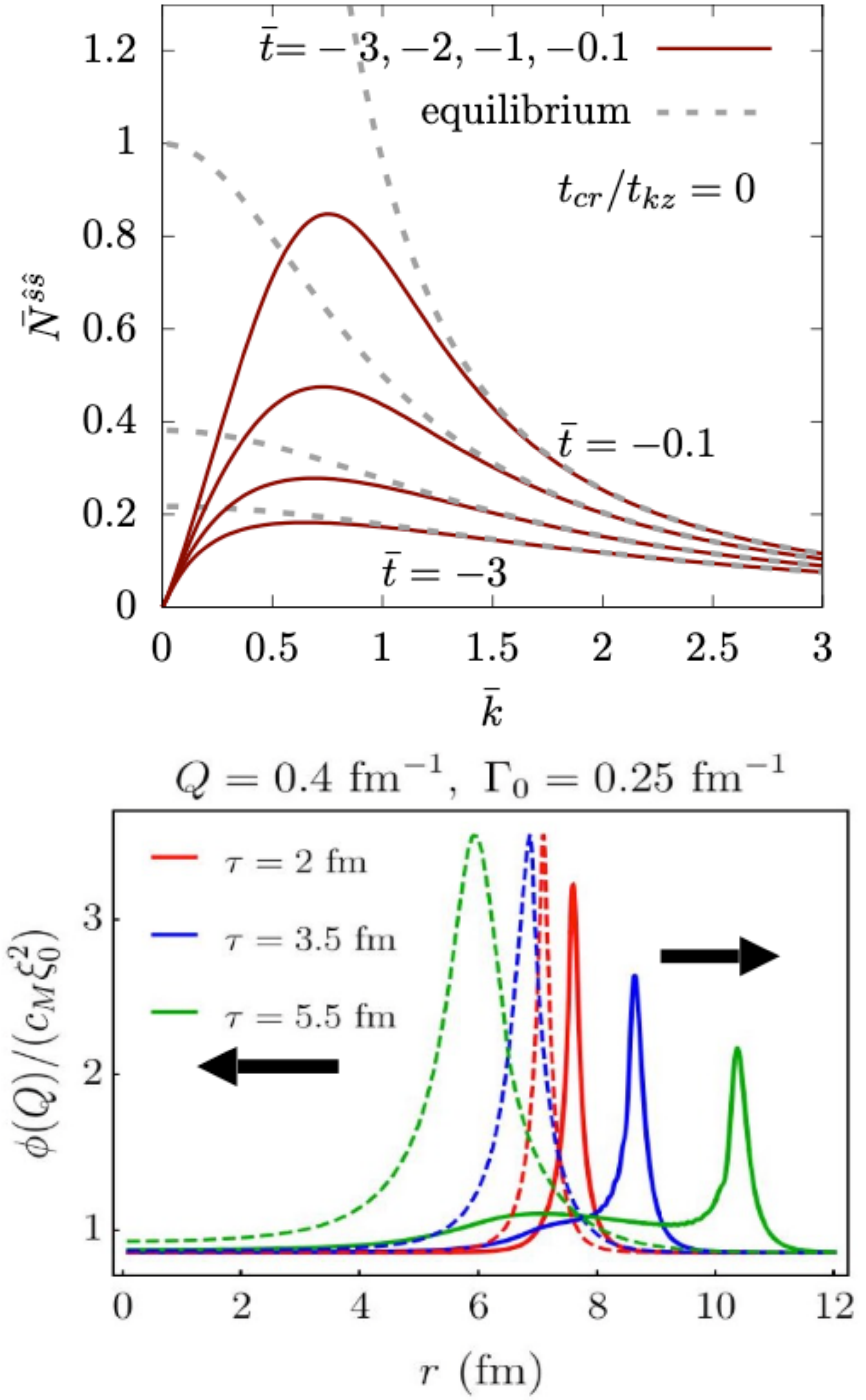

Akamatsu, Teaney, Yan, Yi, [1811.05081]

Bjorken medium

2+1D medium

K. Rajagopal et al. [1908.08539]

L. Du et al. [2004.02719]

SOFTENING & CLUSTERING AT THE FIRST-ORDER PHASE BOUNDARY

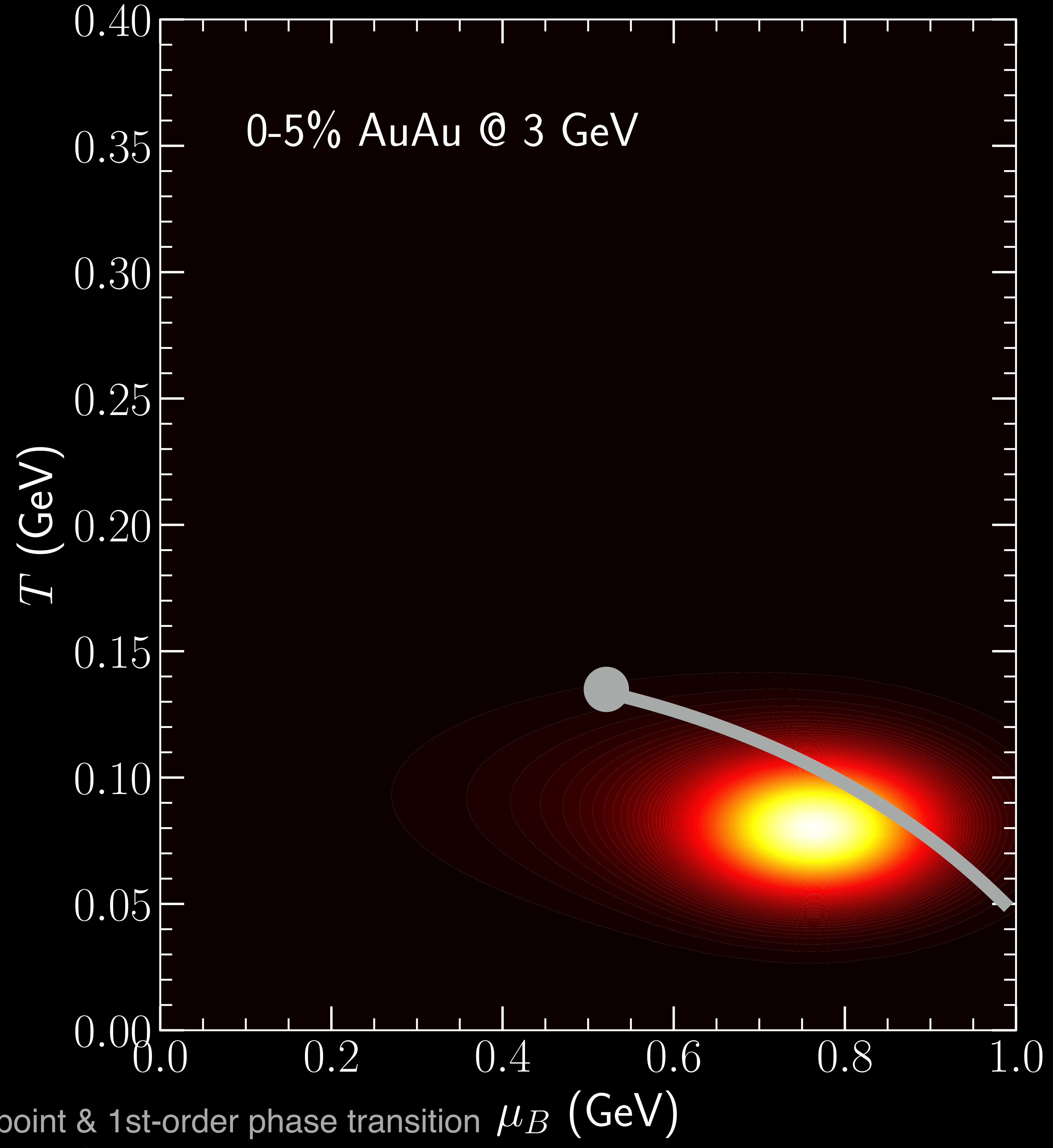

critical point & 1st-order phase transition line are only for illustration purposes

SOFTENING AT THE FIRST-ORDER PHASE BOUNDARY

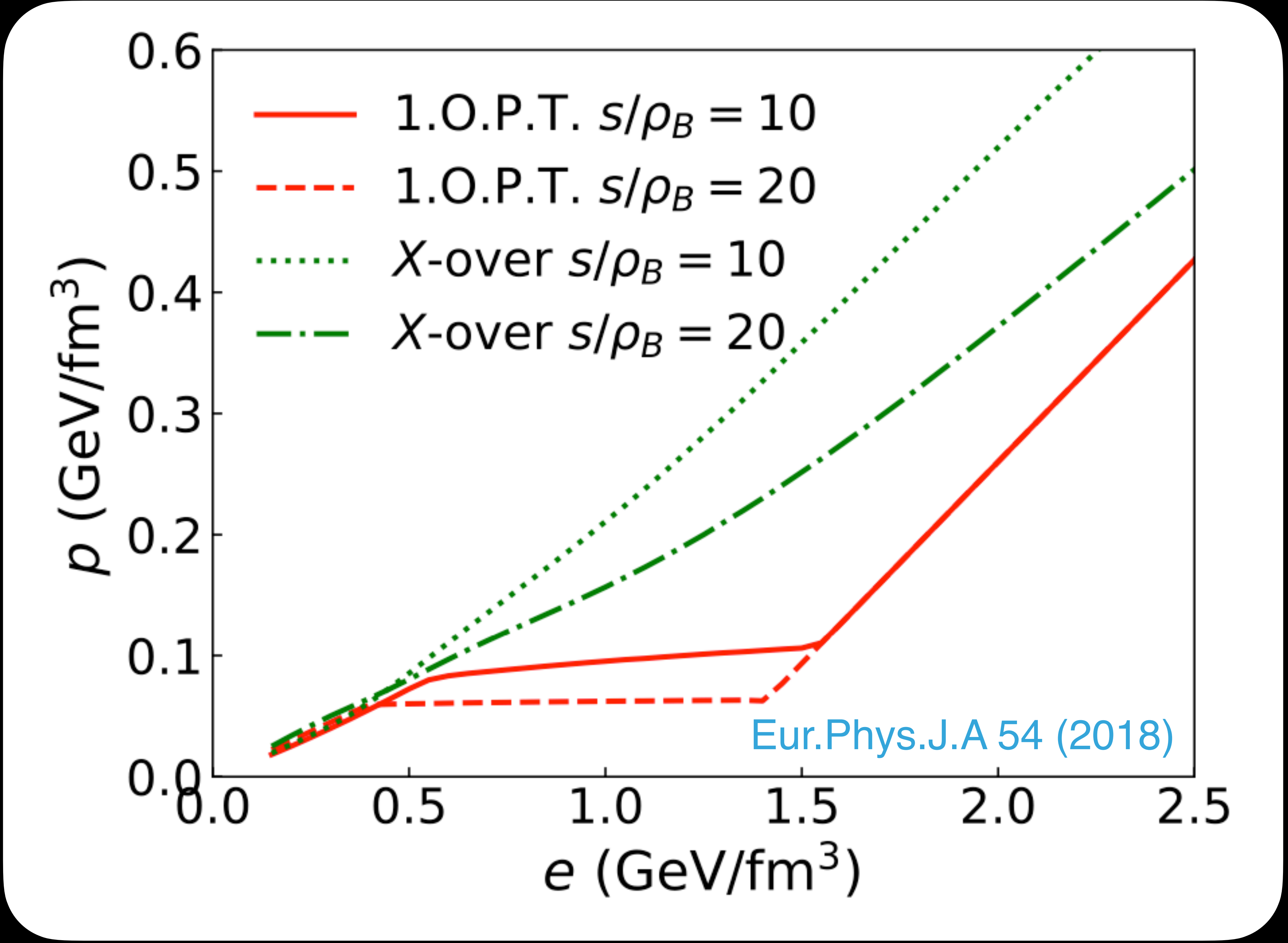

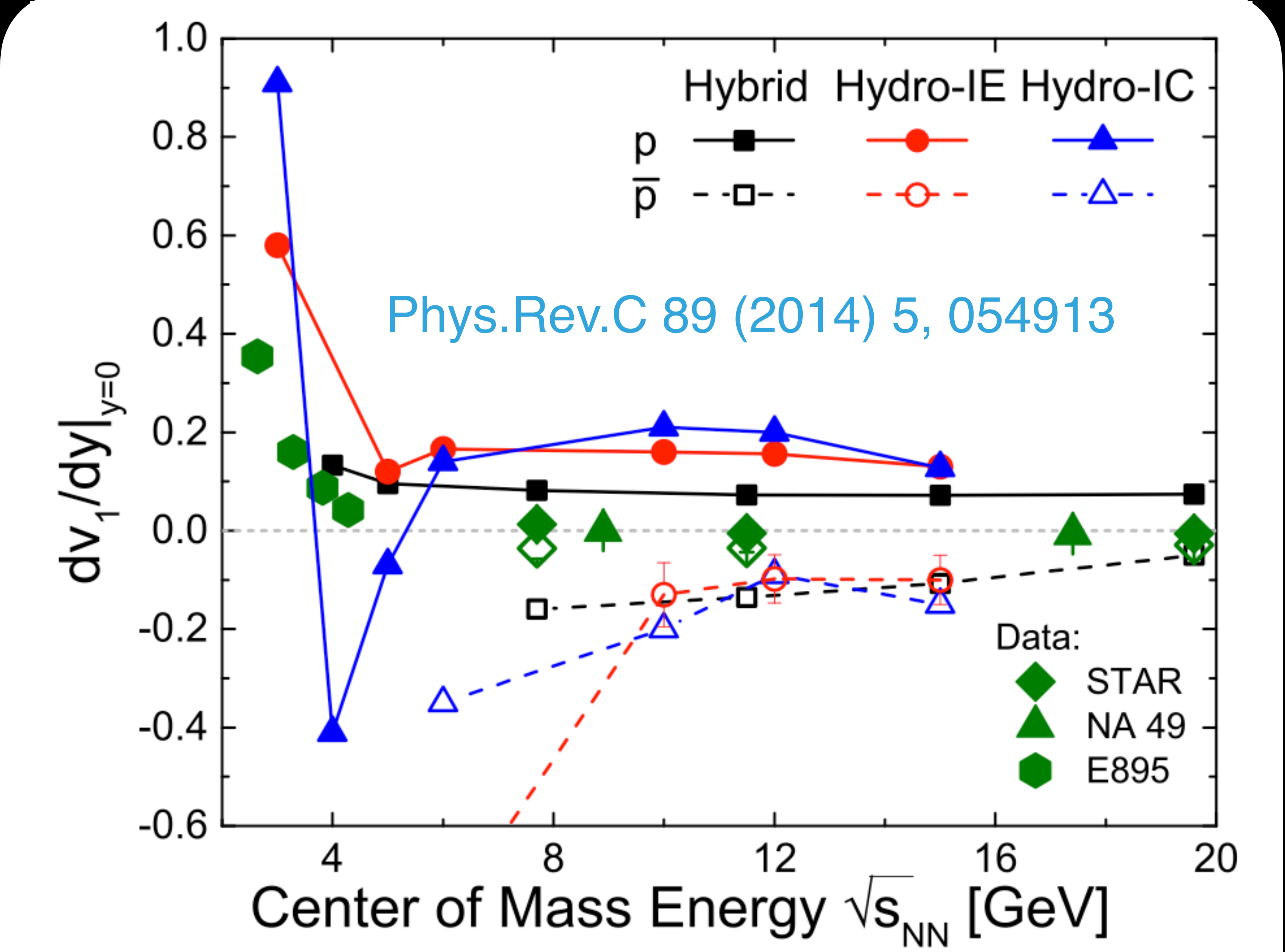

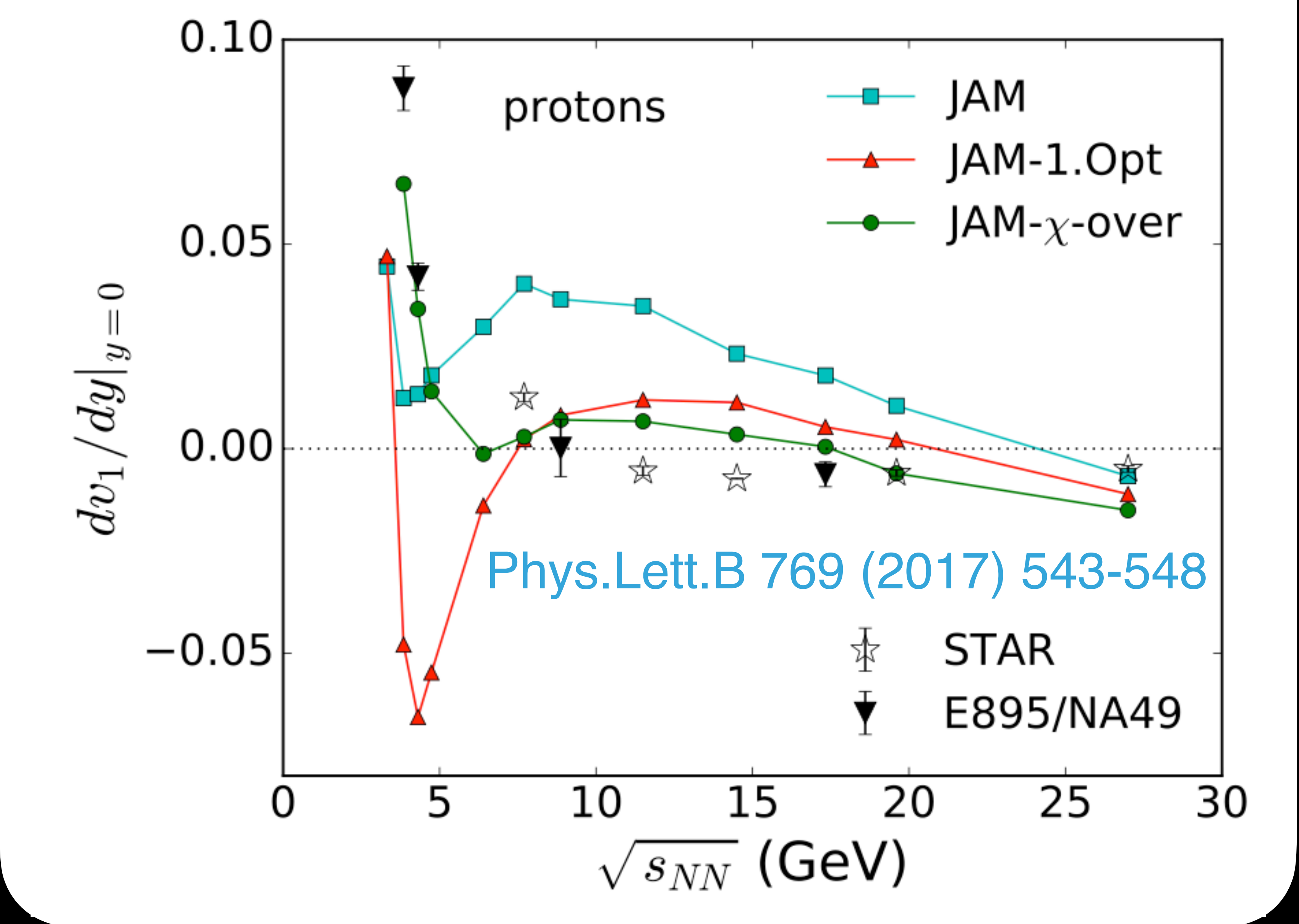

- The slope of protons' direct flow is sensitive to the softening in EOS but also many other factors

CLUSTERING AT THE FIRST-ORDER PHASE BOUNDARY

J. Randrup, Phys. Rev. C79, 054911 (2009)

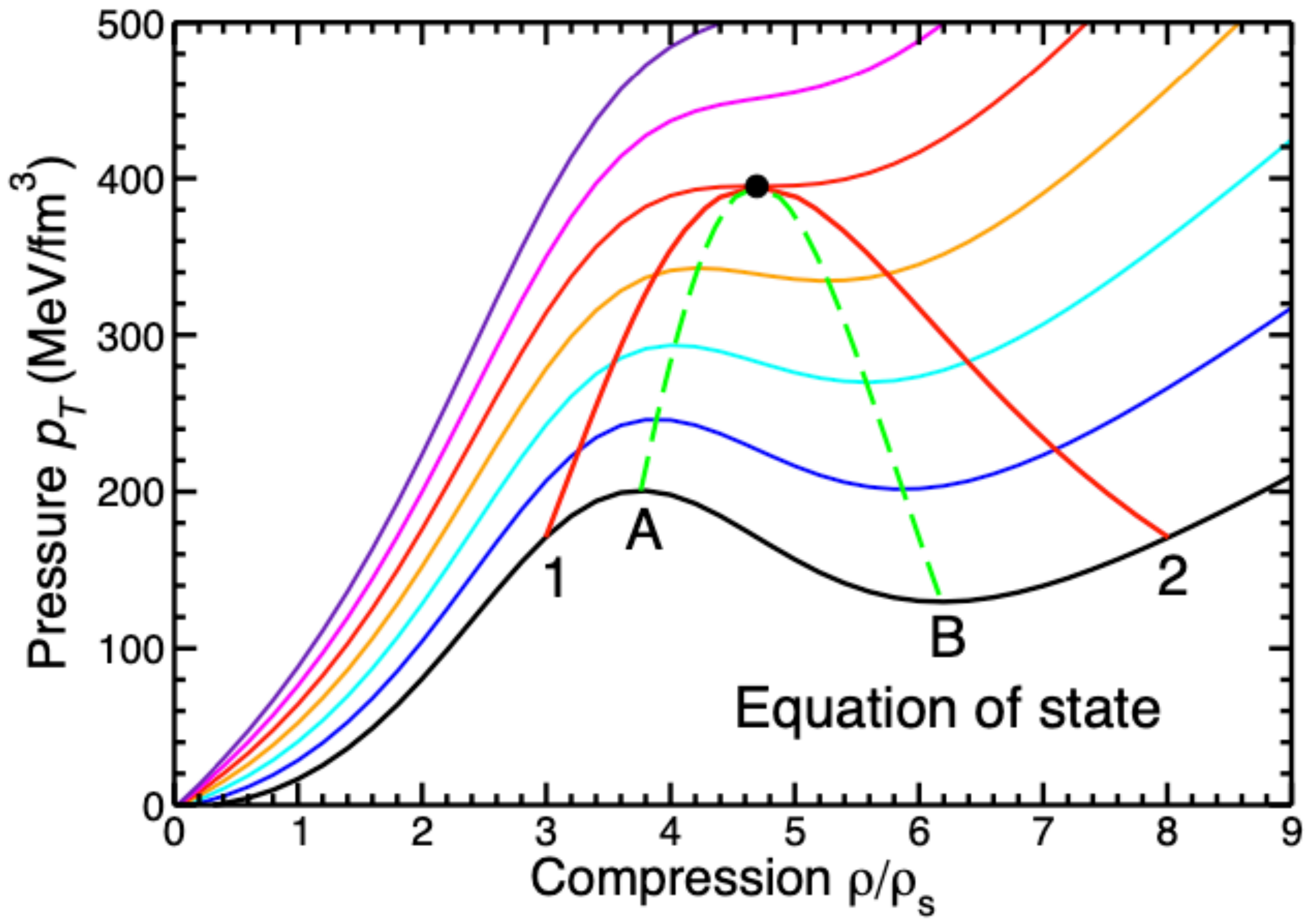

https://en.wikipedia.org/wiki/Spinodal_decomposition

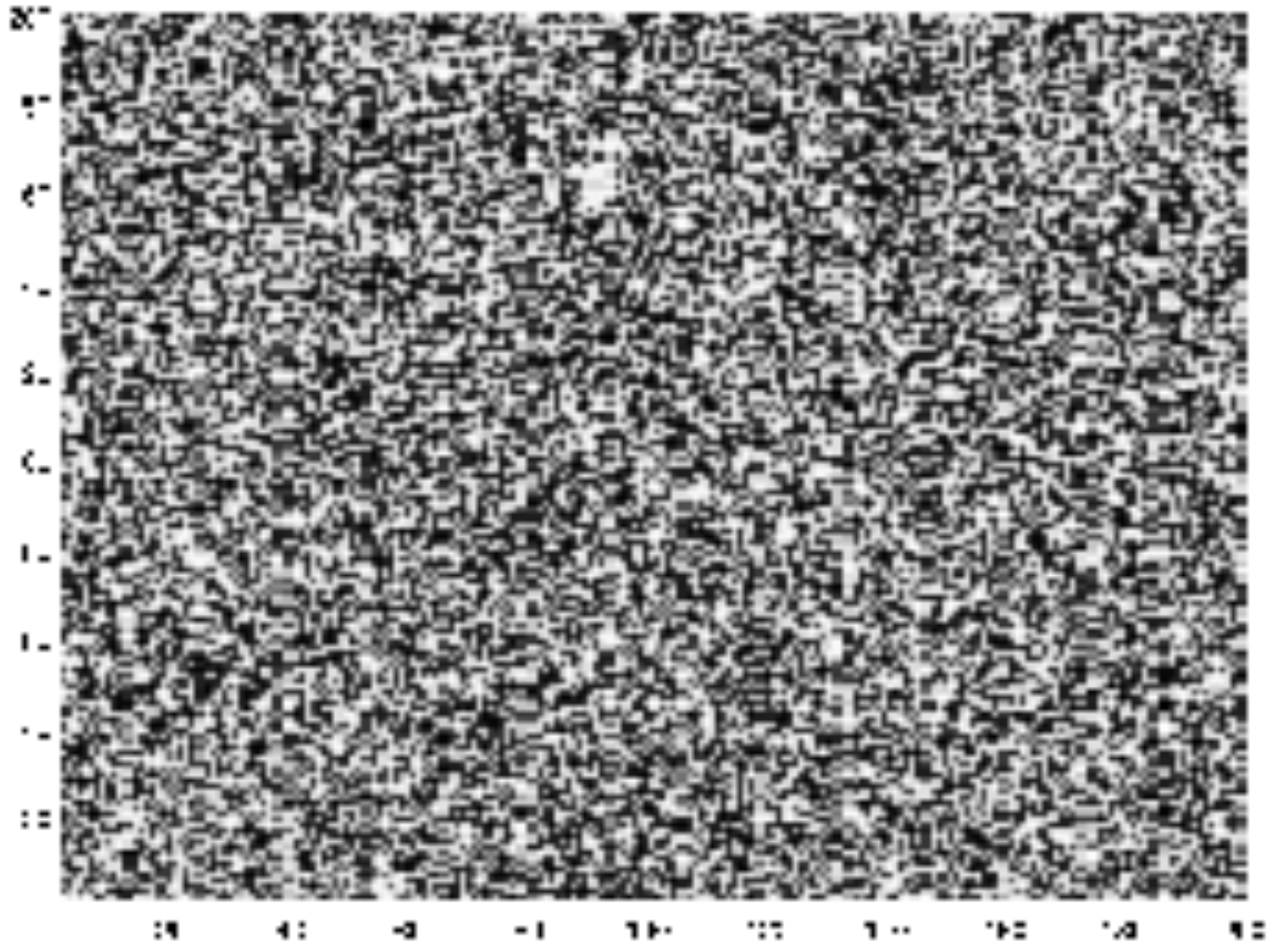

J. Randrup, Phys. Rev. C79, 054911 (2009)
J. Steinheimer and J. Randrup, Phys. Rev. Lett. 109, 212301 (2012)
S. Pratt, Phys. Rev. C96, 044903 (2017)

$$P(r) = P_0(\varepsilon(r), \rho(r)) - a^2 \frac{\varepsilon_s}{\rho_s^2} \rho(r) \nabla^2 \rho(r)$$

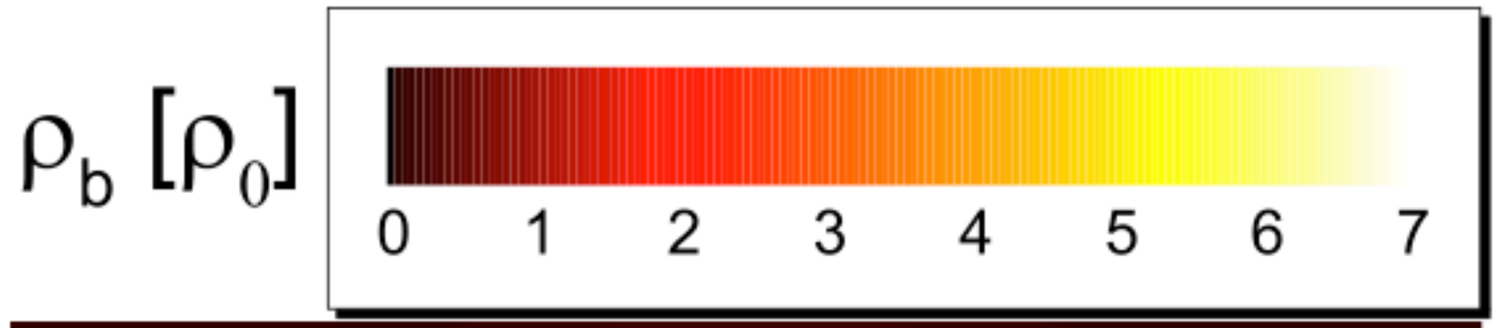

J. Steinheimer, J. Randrup and V. Koch, Phys. Rev. C89, 034901 (2014)

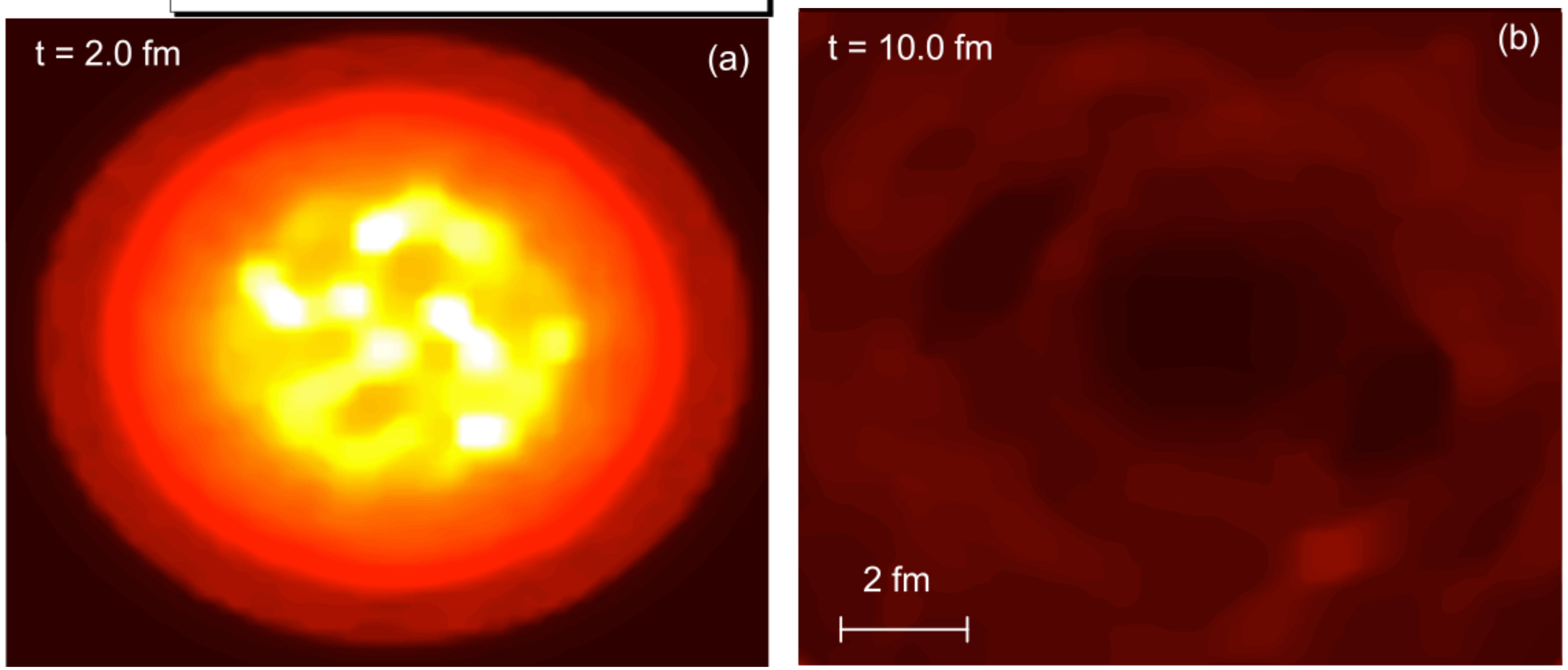

POSSIBLE SIGNALS OF A CRITICAL POINT

STAR, arXiv:2001.02852

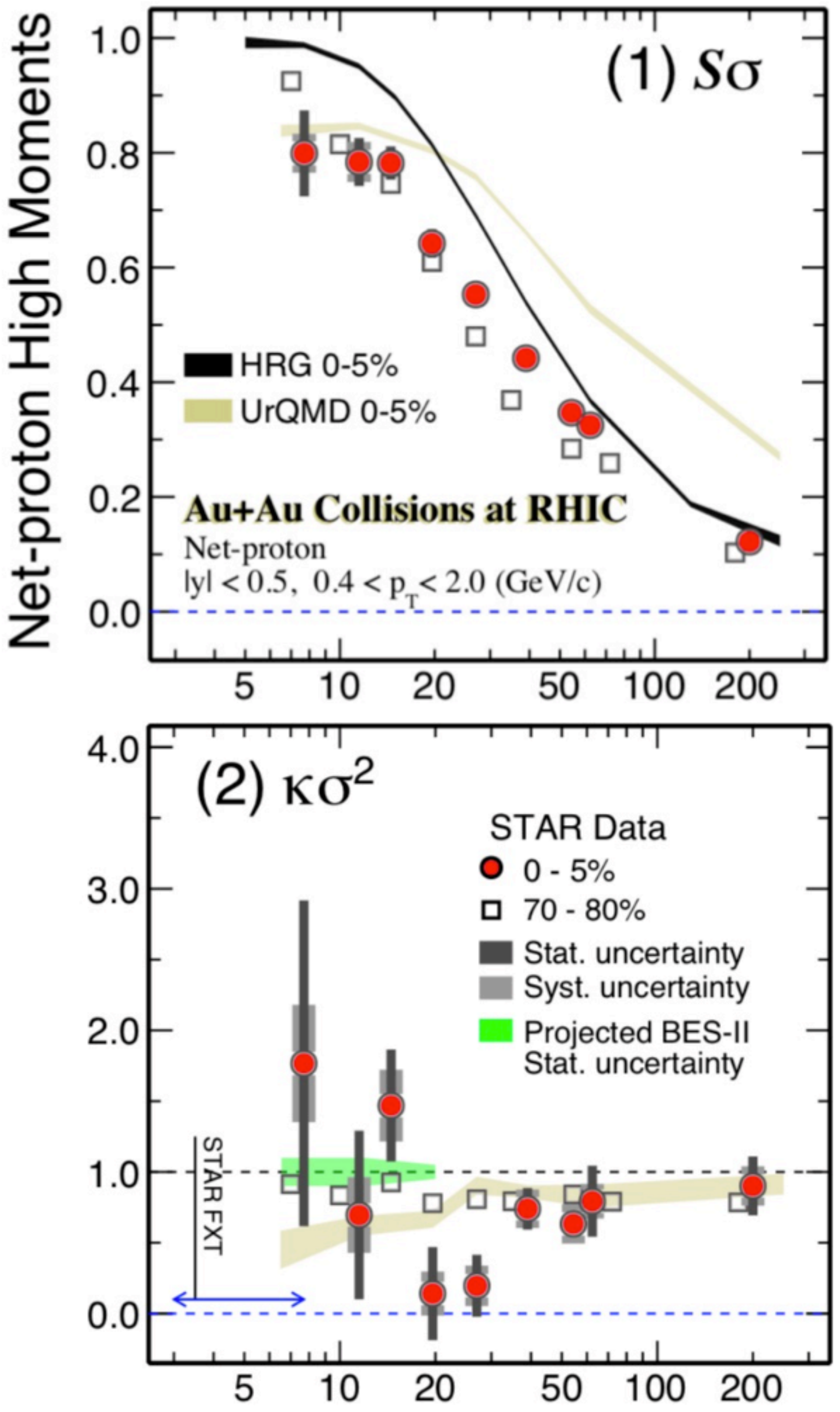

D. Oliinychenko, arXiv:2003.05476

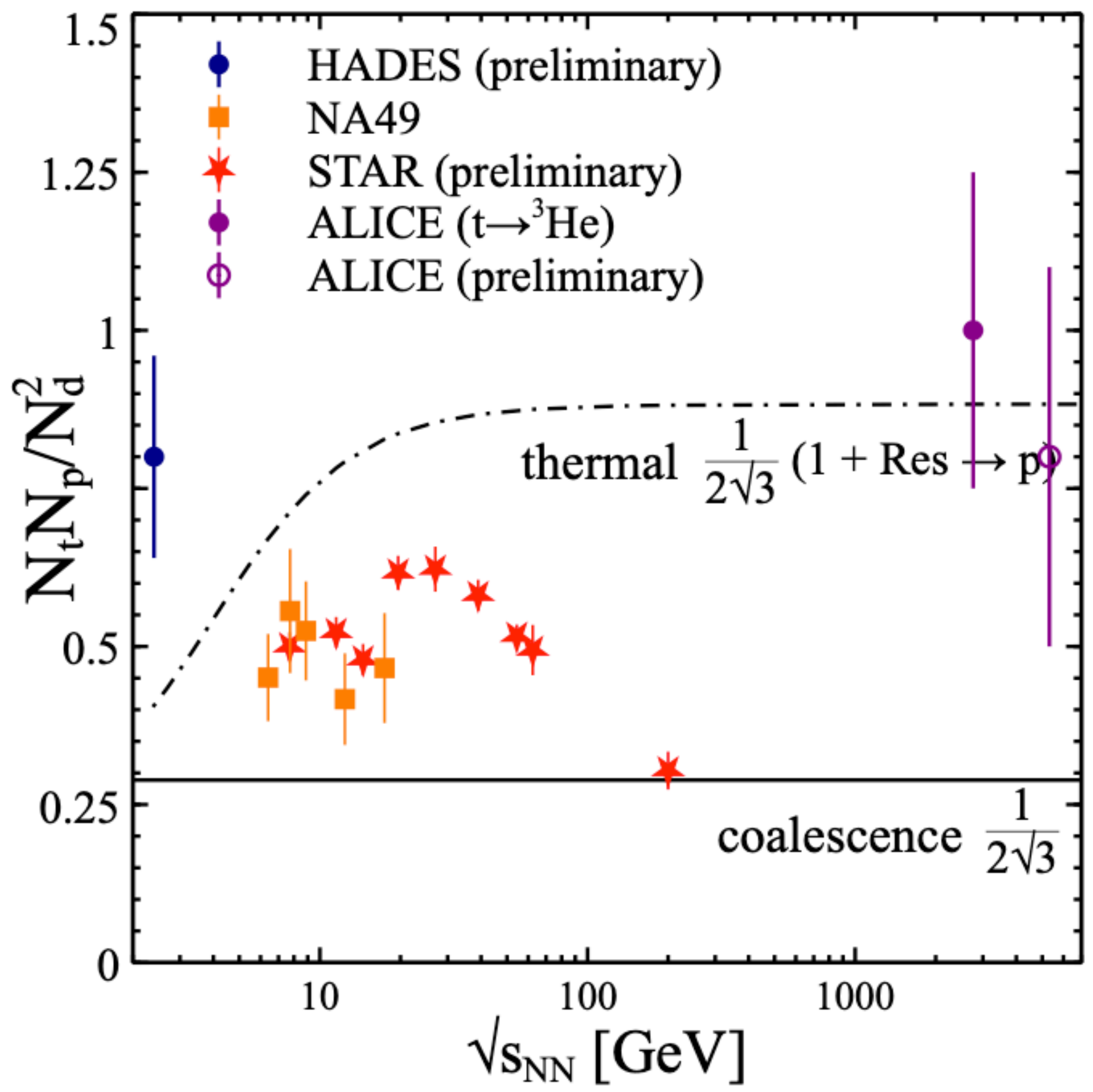

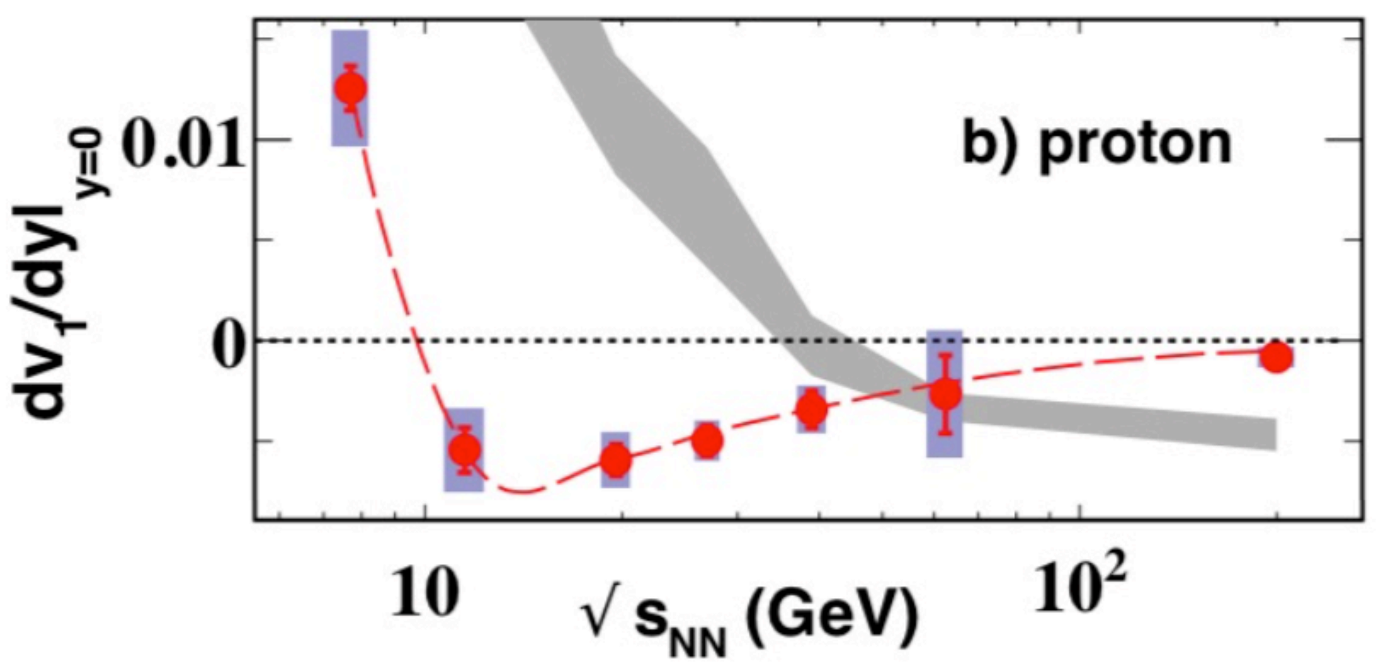

STAR, Phys. Rev. Lett. **112**,162301 (2014)

R. A. Lacey, Phys. Rev. Lett. **114**,142301 (2015)

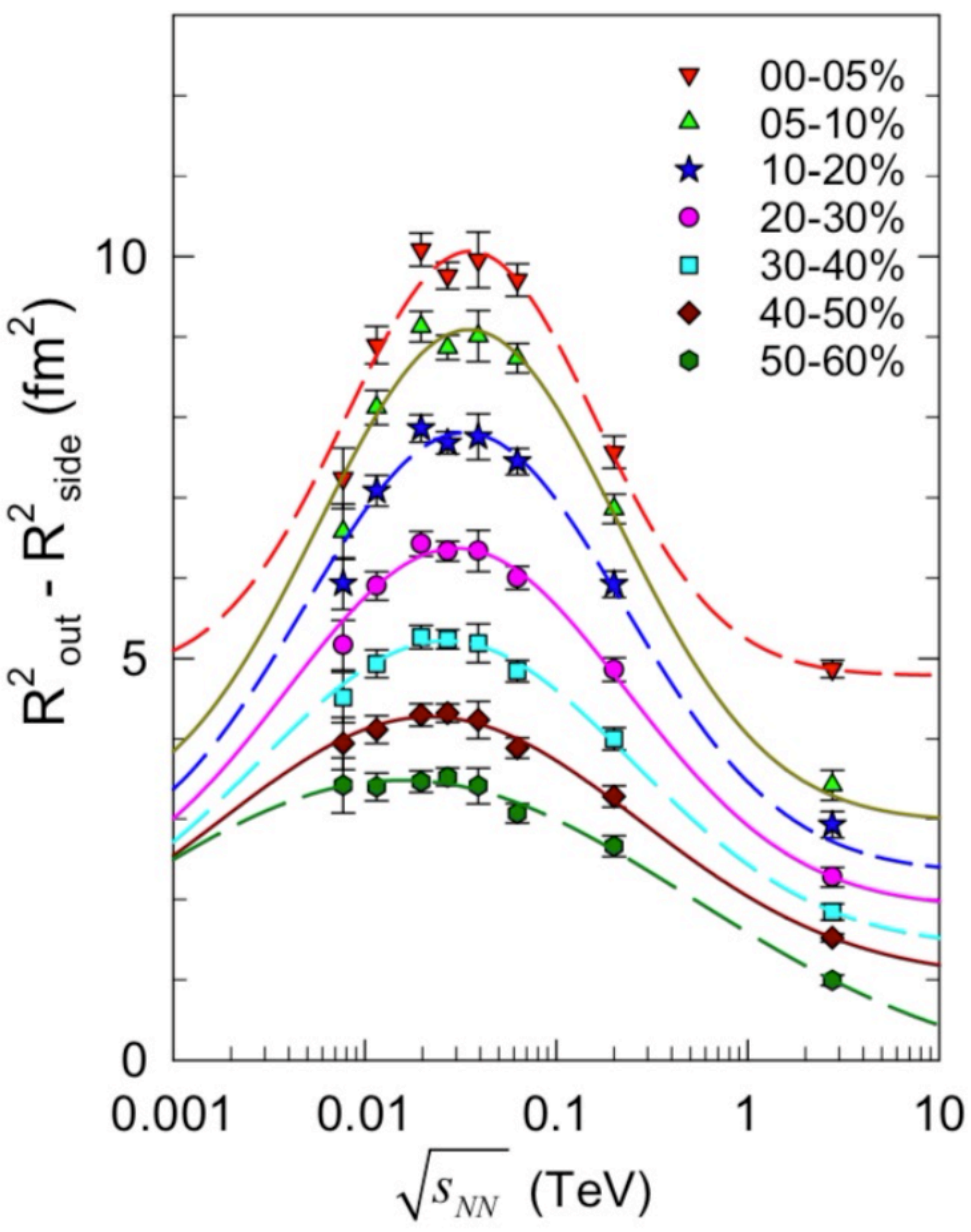

compiled by A. Sorensen

- Need to have a consistent theory description!

SUMMARY

- We developed an effective dynamical framework to understand particle production and flow in relativistic heavy-ion collisions in the RHIC Beam Energy Scan (BES) program

    First principle inputs from lattice QCD for EoS

    Elucidating the initial baryon stopping, charge diffusion, and transport properties of QGP in a baryon rich environment

- Emergent theory progresses have been evolving QCD critical phenomena to a quantitative era

    Systematically study the phase structure (critical point & 1st-order phase transition) of hot QCD matter with RHIC BES II

BEST COLLABORATION

AN OPEN SOURCE FRAMEWORK CONNECTING RHIC BES II